University College of Southeast Norway

Miniature Highly Sensitive Ultrasound Doppler Transducers

Author:

Per Kristian Bolstad

Supervisor:

Lars Hoff

The University College of Southeast Norway –
Faculty of Technology, Natural Sciences and Maritime Sciences –

Department of Micro and Nano Systems Technology

Master in Micro and Nano Systems Technology

July 2017

Abstract

The ultrasound transducer is considered a critical and important part of any ultrasonic measurement system. The transducer is the part of the system that transmits and receives soundwaves by converting electrical energy into acoustic energy and vice versa.

The study in this thesis mainly focused on the development of single element transducers. Transducers were designed, fabricated and characterized. Mid-frequency, 6 MHz, single element transducers were fabricated at the HSN Ultrasound Laboratory. High-frequency, 20 MHz single element transducers were fabricated in the Biomedical Research Center at University of Southern California. Transducers were simulated in one-dimensional circuit models and finite element models for comparison and evaluation of results. Fabricated transducers were characterized by electrical impedance measurements, pulse-echo measurements and beam profile measurements.

Fabrication steps for mid- and high-frequency transducers have been discussed in detail. New and common fabrication designs have been presented where the main optimization factor has been on sensitivity. High sensitivity transducers with a broad bandwidth could find applications in Doppler measurements and Pulse-echo imaging.

Acknowledgements

Table of Contents

List of Figures

List of Tables

1 Introduction

1.1 Background

Ultrasound techonology involves the use of sound waves in the frequency range abouve the human audible range. The field of application for ultrasound is vast, from communication [1] [2], nondestructive testing [3], and most notably, in medicine [4]. The many advantages that ultrasound can offer have enabled it to become a valuable diagnostic tool in a variety of medical disciplines. One of the diagnostic applications of ultrasound is Doppler measurements.

Shigeo Satomura is credited with the earliest development of an ultrasonic Doppler device [8] [9]. Doppler measurements are a common diagnostic technique used in ultrasound to detect blood flow or muscle movement, to assess the state of blood vessels and functions of organs. The echoes scattered by red blood cells carry information about the velocity of the blood. The same transducer used for the insonification (or a separate receiver) can detect these echoes

The Doppler shift frequency is given by [4]

$$f_D = \frac{2v cos(\theta) f}{c} \tag{1-1}$$

Where c is the sound velocity in blood, normally set to 1540 m/s. v is the velocity of the blood flow, which is assumed uniform, θ is the angle between the acoustic axis and the velocity vector, and f is the center frequency of the transducer. The equation above can be rearranged to solve for the blood velocity for a given Doppler frequency f_D.
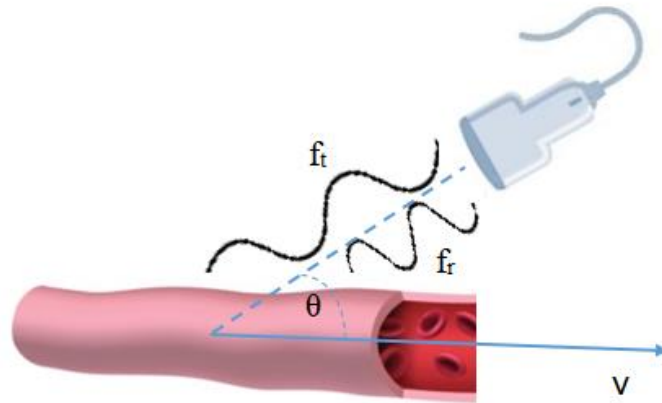
Figure 1.1 – Illustration of the blood flow measurement. The echoes scattered by red blood cells carry information about the velocity of the blood, i.e. the Doppler shift. The transducer is positioned at an angle between the acoustic beam and the direction of the blood flow.

A Doppler shift occurs twice: first when the ultrasound beam hits the moving blood cells and second when the echoes are reflected back by the moving blood cells. The reflected signals are weak so the ultrasound transducer has to have high sensitivity in order to detect the signals.

An ultrasound system, essentially, consists of a transducer, transmitter pulse generator, compensating amplifiers, the control unit for focusing, digital processors and systems for display [7]. The ultrasonic transducer has been identified to be the most critical component of the measurement system [33]. The transducer is the part of the system that transmits and receives soundwaves by converting electrical energy into acoustic energy and vice versa. For Doppler applications, the transducer should be optimized for high sensitivity and a narrow beam profile.

This thesis presents the development of ultrasound transducers, which may be used for Doppler measurements. Single element transducers optimized for high sensitivity, have been designed, fabricated and characterized. Different designs has been presented where the choice of materials and packaging have been carefully considered.

For extravascular applications, 6 MHz mid-frequency frequency transducer has been fabricated. For intravascular applications, high frequency 20 MHz transducers have been fabricated. High frequency transducers have been fabricated at the Biomedical Research Center at the University of Southern California. One of the objectives for this

was to learn about the fabrication steps to make a high frequency transducer. Hence, a detailed description of the fabrication steps is presented.

1.2 Thesis Objectives

The aim is to make miniature highly sensitive single element transducers for combined pulse-echo and Doppler measurements. The primary challenge is to make the transducers as small as possible, including connections and encapsulation, and yet achieve excellent sensitivity and a well defined beam pattern. At least two different transducers shall be made. One mid-frequency transducer, 5 to 10 MHz, this shall be pushed as high as achievable in the HSN ultrasound lab. The second will be a high frequency version, 20 MHz, to be made at the Ultrasound Transducer Resource Center (UTRC) at the University of Southern California (USC). The intended application area of the high frequency transducer is intravascular ultrasound.

The primary purpose of the high frequency transducer is to perform Doppler measurements in blood. The secondary purpose is to detect the vessel wall by means of pulse-echo measurements. Sensitivity will be the primary optimization parameter in this project, but the transducer shall also be able to use pulse-echo measurements to create B-mode or M-mode background images. The bandwidth requirement somewhat relaxed compared to an optimized imaging transducer, the target is tentatively set at 50% relative bandwidth. Small size is required. For the high frequency transducer, the footprint shall be max 2 x 2 mm and thickness 1.5 mm after packaging and connecting. These limits shall be pushed to as small as achievable, and will depend on frequency. A circular shape would be preferred due to the symmetric beam pattern. However, as fabrication of a circular aperture is difficult in the existing lab equipment, a rectangular shape more feasible.

Tasks:

- Design and modeling
    - Design and model ultrasound transducer stacks in a Mason equivalent circuit model, using the Xtrans software for Matlab.
    - Simulate the structure in FEM, using COMSOL
    - Model the beam pattern in Field II
- Fabrication

- o Evaluate fabrication opportunities, availability of tools and materials.
- o Fabricate a mid-frequency transducer at the HSN lab
- o Connect and encapsulate the transducer. A 3D printed plastic enclosure is proposed as housing.
- o Fabricate the high frequency version of the transducer in UTRC, USC
- Characterization
  - o Test the mid and high frequency transducers using electrical impedance and pulse-echo measurements.
  - o Find sensitivity, pulse shapes and bandwidth from pulse-echo measurements
  - o Measure beam pattern of transducers
- Compare measurements and calculations, comment, explain.

1.3   Thesis Structure

The thesis is organized in the following way. An introduction to Doppler ultrasound, research motivations and the objectives of the thesis is given in Chapter 1. Chapter 2 presents theory related to the ultrasound transducer and equivalent theoretical models. Chapter 3 presents the methods used for simulating the one-dimensional and finite element model, as well as the beam profile. The fabrication and characterization methods are described. The results are given in Chapter 4 with a detailed discussion of the results in Chapter 5. Chapter 6 concludes the work and suggestions to future works are presented. The appendix contains detailed stepwise descriptions of the mid frequency and high frequency transducer fabrication.

Material parameters used for all simulations are listed in 4.1.1. The purpose of this is to collect material data for comparison with results in an organized manner. Fabricated transducers are given reference names in order to systematically refer to them throughout the text.

2 Theoretical Background

2.1 Single Element Ultrasound Transducers

2.1.1 Piezoelectric Element

The piezoelectric effect is a phenomenon in which a material, upon the application of an electrical field, changes its physical dimensions and vice versa. The direct piezoelectric effect refers to the phenomenon in which the application of a stress causes a net electric charge to appear across the electrodes. In the reverse, or inverse effect, a potential difference across the electrodes will induce a deformation of the material. This deformation causes tensile or compressive stresses and strains in the material and is dependent on the direction of the electric field, the direction of which the piezoelectric material is poled and the mechanical clamping of the material.

When the piezoelectric material is subjected to an alternating electric field, the material will vibrate, creating alternate compression and rarefication in the surrounding media, i.e. sound waves. Wavelength is given mathematically as:

$$\lambda = \frac{c}{f} \tag{2-1}$$

where c is the speed of sound in the medium and f is the frequency of the wave. The resonance frequencies of the piezoelectric element can be found by considering the element as two independent vibrators, one acoustic port in the front and one in the back [4].

$$f_0 = n \frac{c_p}{2t} \tag{2-2}$$

Where n is an odd integer, c_p is the speed of sound in the piezoelectric and t is the thickness of the piezoelectric. Combining Equations 2.1 and 2.2, and rearranging shows that resonance occurs when t is equal to odd multiples of one-half wavelength. λ_p is the wavelength in the piezoelectric material.

$$t = n \frac{\lambda_p}{2} \tag{2-3}$$

Piezoelectric materials occur naturally, yet these are rarely used in diagnostic ultrasound due to their weak piezoelectric properties. For this purpose, a variety of

ferroelectric materials with stronger piezoelectric coupling are available today. A description of the some of the piezoelectric properties follows.

The electromechanical constitutive equations for a linear piezoelectric material in the stress-charge form are [10]:

$$T = [C^E]S - [e]^t E \qquad\qquad \textbf{(2-4)}$$

$$D = [e]S + [\varepsilon^s]E \qquad\qquad \textbf{(2-5)}$$

where T is the stress vector, S is the strain vector, D is the electric displacement vector and E is the electric field vector. C is the elasticity matrix where the superscripted E indicate that the values were measured with a constant electric field across the material. e is the piezoelectric charge coefficient, where superscript t indicate that the matrix is transposed. ε is the dielectric matrix where superscript S (inside the bracket of Equation 2.5) indicate that the constant were measured at constant or zero strain.

Piezoelectric materials will in most cases have a crystal structure with symmetry of hexagonal 6mm class. If the material is poled along one of the axis of symmetry, the material will become transversely isotropic, meaning that all directions perpendicular to this axis will be equivalent. In this case, the elasticity, dielectric, and piezoelectric charge coefficient matrices for a polarized, linear piezoelectric material are given according to Equation 2.6, Equation 2.7 and Equation 2.8, respectively [11].

$$C^E = \begin{bmatrix} C11^E & C12^E & C13^E & 0 & 0 & 0 \\ C13^E & C22^E & C13^E & 0 & 0 & 0 \\ C13^E & C13^E & C33^E & 0 & 0 & 0 \\ 0 & 0 & 0 & C44^E & 0 & 0 \\ 0 & 0 & 0 & 0 & C55^E & 0 \\ 0 & 0 & 0 & 0 & 0 & C66^E \end{bmatrix} \qquad \textbf{(2-6)}$$

$$\varepsilon = \begin{bmatrix} \varepsilon_{11} & 0 & 0 \\ 0 & \varepsilon_{22} & 0 \\ 0 & 0 & \varepsilon_{33} \end{bmatrix} \qquad \textbf{(2-7)}$$

$$e = \begin{bmatrix} 0 & 0 & 0 & 0 & e_{15} & 0 \\ 0 & 0 & 0 & e_{15} & 0 & 0 \\ e_{31} & e_{31} & e_{33} & 0 & 0 & 0 \end{bmatrix} \qquad \textbf{(2-8)}$$

Piezoelectric materials with high dielectric constants permit the electrical impedance of the elements to better match the electrical impedance of the processing electronics.

One of the most important material parameters to consider for fabricating a transducer is the electromechanical coupling coefficient, k. The electromechanical coupling coefficient is the capability of the material to convert electric energy to mechanical energy and vice versa. This coefficient depends on material geometry of the piezoelectric element. When the lateral dimensions (width) of the transducer is much larger than the thickness, the thickness mode electromechanical coupling coefficient k_t applies.

2.1.2 Acoustic Impedance Matching

Another important material parameter to consider is the acoustic impedance. The acoustic impedance of the piezoelectric should match the impedance of the load medium to achieve optimal energy transmission. However, the piezoelectric material usually has a charachteristic acoustic impedance ~30 MRayl, while the load material, being water or biological tissue, has characteristic impedance around 1.5 MRayl [20]. This causes strong reflections at the interface, limiting the transmission of acoustic energy out from the piezoelectric plate, reducing the bandwidth of the transducer. This is compensated by adding acoustic matching layers between the piezoelectric and the load. The characteristic acoustic impedance for a material is equal to the acoustic impedance of a plane wave,

$$Z = \rho c \tag{2-9}$$

where Z is the characteristic acoustic impedance, ρ is density and c is longitudinal wave velocity in the medium of consideration.

The performance of a transducer can be improved by matching the acoustic impedance towards the front of the transducer with the use of matching layers. Based on transmission line theory, 100% transmission occurs for a monochromatic plane wave when the thickness of the matching layer is a $\lambda_m/4$. This layer has the acoustic impedance Z_m where λ_m is the wavelength in the matching layer material [12].

$$Z_m = (Z_p Z_l)^{1/2} \tag{2-10}$$

For a wideband transducers, Desilets, et al. [13] found that effectively lower target values for the matching layer impedances could be derived based on the KLM equivalent circuit model. For a single matching layer, the matching layer impedance is:

$$Z_m = (Z_p Z_l^2)^{1/3} \qquad\qquad \textbf{(2-11)}$$

For two matching layers, the acoustic impedances of the two layers should be:

$$Z_{m1} = (Z_p^4 Z_l^3)^{1/7} \qquad\qquad \textbf{(2-12)}$$

$$Z_{m2} = (Z_p Z_l^6)^{1/7} \qquad\qquad \textbf{(2-13)}$$

With an air-backed transducer, most of the acoustic energy that reaches the back of the piezoelectric element will be reflected into the forward direction due to acoustic impedance mismatch between the piezoelectric material and air. The reflected energy will reverberate inside the piezoelectric element, causing a ringing effect, which lengthens the pulse duration. This is undesirable since a longer pulse duration will affect the spatial resolution.

Spatial resolution is the ability the transducer to distinguish two points, separate in space. Higher resolution means points at smaller distance can be separated. Axial resolution is resolution along the direction parallel to the beam and is not affected by depth of imaging, but the pulse duration. Lateral resolution is the resolution perpendicular to the beam. The width of the beam determines the lateral resolution, and this width normally increases with depth. The axial resolution of a transducer can be improved from an increase in the bandwidth by using a backing layer, matching layer or by focusing the beam, while the lateral resolution is determined by the frequency, focusing and aperture size.

Backing materials with an acoustic impedance similar to that of the piezoelectric material can be used to damp out the ringing effect and thereby increasing bandwidth. The backing material should not only absorb part of the energy from the vibration of the back face but also minimize the mismatch in acoustic impedance. This suppression of ringing or shortening of pulse duration is achieved by sacrificing sensitivity since the backing material absorbs a large portion of the energy.

8

2.2 Modelling of Single Element Transducers

2.2.1 One-Dimensional Equivalent Model

One-dimensional equivalent circuits can be used to describe the thickness vibration mode of the piezoelectric transducer. Two commonly used equivalent circuits are the Mason's model [14] and the KLM (Krimholtz, Leedom and Matthaei) model [15].

In the KLM and Mason equivalent circuit models, the transducer can be treated as a three-port network of two mechanical ports, representing the front and back surfaces of the transducer and one electrical port, representing the electrical connections. The governing equations for the two models [16] are shown in Table 2.1. Figure 2.1 [16] shows the equivalent circuits.

Table 2.1 – Governing Equations For Mason and KLM Model

Mason Model		KLM Model	
$Z_T = iZ_0 \tan\left(\frac{\Gamma t}{2}\right)$	(2-14)	$M = \frac{h_{33}}{\omega Z_0}$	(2-17)
$Z_s = -iZ_0 \csc(\Gamma t)$	(2-15)	$X_1 = iZ_0 M^2 \sin(\frac{\Gamma t}{2})$	(2-18)
$N = C_0 h_{33}$	(2-16)	$Z_{TL} = Z_0 \left[\frac{Z_L \cos\left(\frac{\Gamma t}{2}\right) + iZ_0 \sin\left(\frac{\Gamma t}{2}\right)}{Z_0 \cos\left(\frac{\Gamma t}{2}\right) + iZ_L \sin\left(\frac{\Gamma t}{2}\right)}\right]$	(2-19)
		$Z_{TR} = Z_0 \left[\frac{Z_R \cos\left(\frac{\Gamma t}{2}\right) + iZ_0 \sin\left(\frac{\Gamma t}{2}\right)}{Z_0 \cos\left(\frac{\Gamma t}{2}\right) + iZ_R \sin\left(\frac{\Gamma t}{2}\right)}\right]$	(2-20)
		$\phi = \frac{1}{2M} \csc\left(\frac{\Gamma t}{2}\right)$	(2-21)
		$Z_0 = A\sqrt{\rho c_{33}^D}$	(2-22)
		$\Gamma = \omega \sqrt{\frac{\rho}{c_{33}^D}}$	(2-23)
		$C_0 = \frac{\varepsilon_{33}^S A}{t}$	(2-24)
		$h_{33} = k_t \sqrt{\frac{c_{33}^D}{\varepsilon_{33}^S}}$	(2-25)
		$k_t^2 = \frac{h_{33}^2 \varepsilon_{33}^S}{c_{33}^D}$	(2-26)

ε_{33}^S is the clamped complex dielectric constant. c_{33}^D is the open circuit complex elastic stiffness. k_t is the complex electromechanical coupling coefficient. Z_0 is the characteristic impedance of the piezoelecetric. ρ is the density. Γ is the wave number in the thickness direction. ε_{33}^S is the relative dielectric constant in the thickness direction. A and t is the area and thickness of the PZT, respectively. N and ϕ is the turns ratio for the Mason and KLM model, respectively. Z_L and Z_R is the load impedance on the left and right acoustic ports.
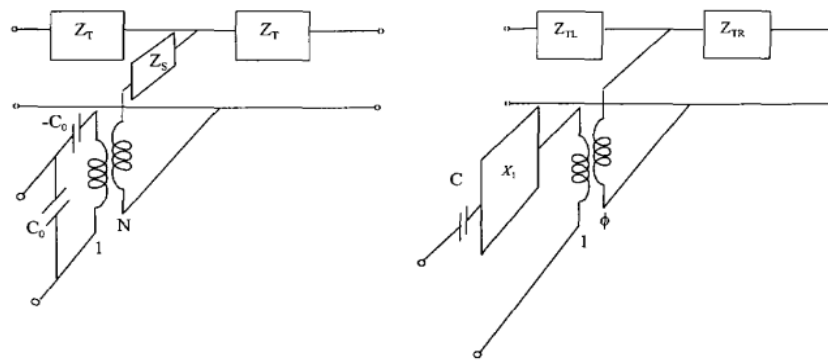
Figure 2.1 –Mason (left) and KLM (right) equivalent circuit model of a piezoelectric transducer.

xTrans [17] is a MATLAB (MathWorks Inc. Natick, MA) program developed at the Department of Circulation and Medical Imaging at NTNU. This program makes use of the Mason model and was used to study the mid- and high-frequency transducers. PiezoCAD (Sonic Concepts. Bothell, WA. Version 3.0) is a commercial transducer modeling software that makes use of the KLM model. PiezoCAD was used to study the high-frequency transducers.

2.2.2 Finite Element Method

The finite element method, FEM for short, is a numerical technique for finding approximate solutions to partial differential equations. The structure is divided into smaller, finite elements. The equations that model the finite elements are then assembled into a larger system of equations that models the entire problem. COMSOL Multiphysics 5.2a (COMSOL Inc. Burlington, MA), from here referred to as COMSOL, is a simulation software for to solving complex partial differential equations in the finite element method [21].

2.2.3   Field II

Field II [18][19] is a Matlab program developed by Jørgen Jensen at the Technical University of Denmark. The program can simulate all kinds of ultrasound transducers and associated images. Field II consists of a C program and a number of Matlab m-functions that are used to call this program. Three types of m-functions are used; for initializing the program, for defining and manipulating transducers and for performing calculations.

3 Methods

3.1 Design and Fabrication of Mid-Frequency Single Element Transducers

The ultrasound lab at HSN is equipped with tools and materials to fabricate and characterize ultrasound transducers in a lower to mid frequency range (1MHz to 8MHz). Figure 3.1 illustrates the procedure for simulating, fabricating and characterizing an ultrasound transducer. The process for developing a transducer can be considered an optimization cycle as the figure indicates. First, a transducer is designed according to Equations 2-10 – 2-13. One-dimensional Mason model and FEM simulations indicate the performance of the transducer. Field II can be used to simulate the beam profile, and find optimal dimensions of the aperture for the specific applications. Next, a transducer can be fabricated. The transducer lab is equipped to characterize the fabricated (and commercial) transducers by electrical impedance measurements, beam profile measurement and pulse-echo measurements. The characterized transducer can then be compared to simulations. If necessary, the material parameters for the transducer layers can be fitted to yield more realistic simulation results, which in turn can be beneficial to fine-tune the fabrication process to meet required specifications for the transducer.
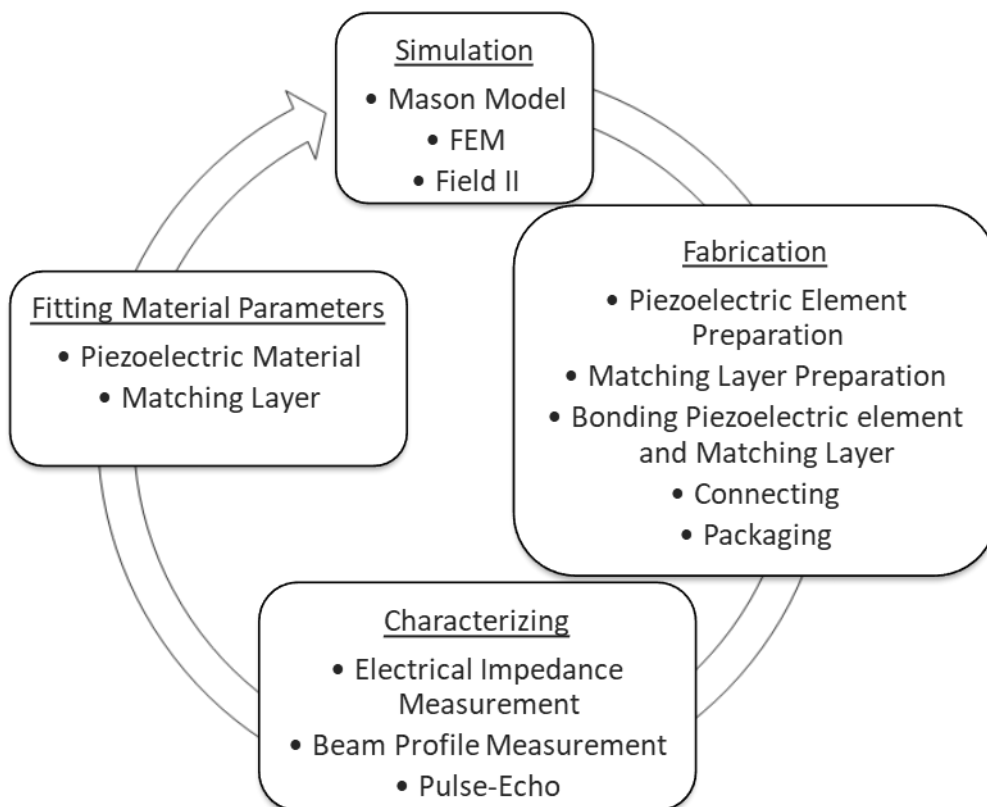
Figure 3.1 - Procedure for developing a mid-frequency ultrasound transducer.

3.1.1 Design Considerations for Mid-Frequency Transducer

The mid-frequency transducer should operate at a center frequency of 6 MHz with a bandwidth of approximately 50%. The aperture was designed to be an unfocused square where the dimensions were dependent on the frequency. The intended purpose of the transducers is to take measurements in blood, yet water will be used as the load for the acoustic measurements. The two liquids have similar acoustic properties, so properties for water were used for all calculations.

Table 3.1 – Acoustic Properties of Loads

	Water	Blood
Speed of Sound [m/s]	1480	1575
Acoustic Impedance [MRayl]	1.48	1.66
Wavelength at 6 MHz [µm]	246.67	262.50

A rule of thumb is to make the aperture size a minimum of 10 times the acoustic wavelength in the load medium in order to obtain a narrow beam. Hence, the minimum aperture size is 2.47 mm in length and width for a square aperture. The transducer aperture size was made approximately 17 times the wavelength in water.

Piezoceramic PZ29 (Ferroperm Piezoveramics A/S. Kvistgaard, DK) was used as the active element in the mid-frequency transducers. Electrical impedance measurement on the piezo ceramic indicated a resonant frequency of 6.7 MHz. The PZT material has good piezoelectric coupling coefficient k_t of 0.524 and high dielectric constants ε_{33} of 1220.

A single matching layer was chosen for the mid-frequency transducers. Two versions of the transducers were fabricated with different matching layers according to Equations 2-10 and 2-11. The materials Eccosorb MF114 and Eccosorb MF112 (Laird N.V. Geel, BE) were used as the matching layers as these materials were readily available in the lab. As described in 2.1.2 regarding maximum power transmission, the thickness of the matching layer was set at $\lambda_m/4$.

Table 3.2 – Acoustic Impedance of Matching Layers

	Acoustic Impedance [MRayl]
Equation X	7.71
Eccosorb MF114	6.54
Equation Y	4.25
Eccosorb MF112	4.91

A bonding layer, e.g. glue, was necessary to bond the piezoelectric element to the matching layer. As this layer is non-conductive and will decrease the sensitivity of the transducer, it should be made as thin as possible.

A model for a housing was designed to allow for free space between the walls of the housing and the piezoelectric element. With this design, the transducer will be air backed and not clamped on the sides of the element, which will result in increased sensitivity.
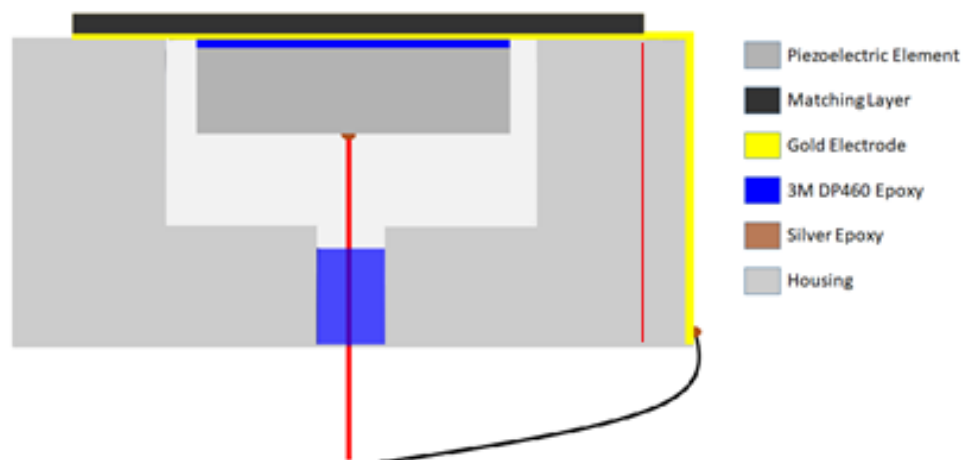
Figure 3.2 – Layers and dimension of mid-frequency transducer

3.1.2   Fabrication of Mid-Frequency Transducers

One of the requirements for this thesis was to accurately document the fabrication steps. To avoid too much detail in this chapter, the complete and detailed description of the fabrication steps were put in in Appendix A.

Piezoelectric material PZ29 was used for the active element in the mid frequency transducers. 4.2 mm * 4.2 mm squares of PZ29 were diced out from a larger sample and cleaned. Two different matching layer materials, Eccosorb MF112 and Eccosorb MF114, were used to make two different versions of the mid-frequency transducer. Matching layers were lapped to the desired thickness and diced into squares of 5.4 mm * 5.4 mm, then cleaned. A plastic housing was designed in the SolidWorks software (Dassault Systems SOLIDDWORKS Corp. Waltham, MA) and 3D printed to house the transducers. The matching layers and the plastic housings were sputtered with chrome as a seed layer and gold as a conductive layer. The gold covered one surface of the matching layer and half of the housing, see Figure 3.2 for reference. One gold plated matching layer was bonded with epoxy (DP460, 3M, Scotch-Weld, Epoxy Adhesive) to one piezoelectric element, with the gold plated side of the matching layer facing the electrode of the piezoelectric element. A copper wire was connected to the back of the piezoelectric element using conductive silver epoxy. The resulting stack (PZ29 bonded to matching layer) was then placed in the housing where the gold plated matching layer had contact with the gold plated housing. Superglue was used to make the bond between the housing and the stack. Another wire was bonded with conductive silver epoxy to the conductive half of the housing. At last, the transducer (stack in housing with wires connected) was placed in a 3D printed probe to perform acoustic measurements.

3.1.3   Fitting Material Parameters

Material parameters from manufacturer are not always correct. A fabricated transducer was compared to the theoretical model to study the accuracy of the material parameters. The material parameters for the PZ29 and Eccosorb MF114 were fitted to match the measured impedance. All fitting was done by manually changing the material parameters from the manufacturer in the Xtrans.

Five square samples of PZ29 with dimensions 4.2 mm • 4.2 mm were compared to check for consistency. The thickness was measured using where three samples measured 318 µm ± 0.5 µm, and two of the samples measured 330µm ± 2 µm. The electrodes on the

top and bottom of PZ29 were inspected using optical microscopy with 1000X magnification. The electrical impedance of the five samples were measured using network analyzer HP 8753D (Agilent Technologies Inc. Philadelphia, PA), as shown in Figure 3.1.1. The measured impedances were compared to the Mason model, using material parameters from the manufacturer. These material parameters were fitted to match the measured elements.

Next, a complete transducer was fabricated and characterized by electrical impedance measurement. The measurement was compared to the Mason model, using fitted material parameters for the piezoelectric. The material parameters for the matching layer was fitted to match the measurement. The material parameters for the bonding layer were kept as they were, based on the assumption that since the bonding layer is thin relative to the matching layer, the matching layer will have most influence.

3.2 High-Frequency Single Element Transducers

High-frequency single element transducers were fabricated at the Biomedical Engineering Laboratory in the Downey Research Center of University of Southern California. The exchange took part in February until April of 2017. During a 2.5-month operation, high frequency single element transducers were designed, simulated and fabricated. Lab training was necessary as the fabrication procedure is entirely different to that of mid-frequency transducer.

Figure 3.3 illustrates the procedure for simulating, fabricating and characterizing the high-frequency transducers. Simulations was used to find the dimension of each layer of the transducer. The standard simulation software in the lab was PiezoCAD, a software program based on the KLM model. This software was used along with the Mason model, COMSOL simulations and Field II to estimate the performance of the designed transducer. Once the transducer was designed in compliance with specifications, the fabrication started. The fabrication of high-frequency transducers was a long and time-consuming process. Due to limited time, the fabricated transducers had to be characterized in the HSN ultrasound lab.
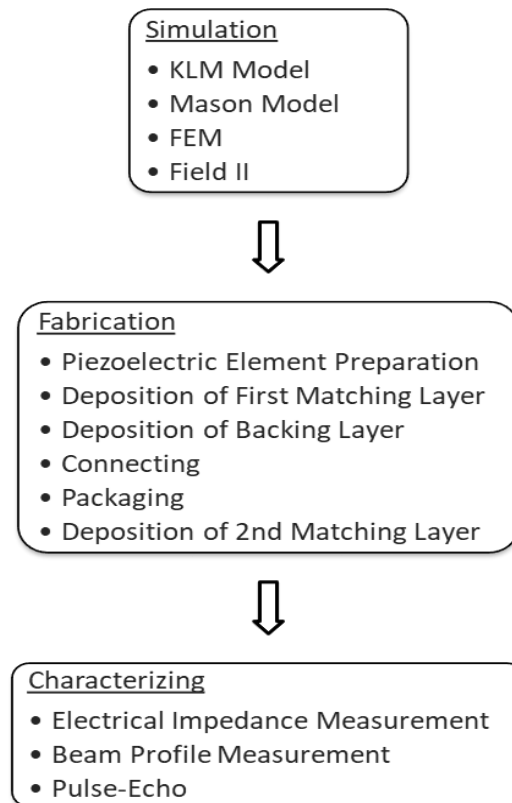
Figure 3.3 – Procedure for Fabricating High Frequency Transducers

3.2.1   Design Considerations for High-Frequency Transducer

The high-frequency transducer was designed to operate at a center frequency of 20 MHz with a bandwidth of approximately 50%. The aperture was designed to be an unfocused square. The wavelength in water at 20 MHz is equal to 75 µm. A rule of thumb is to have the aperture size a minimum of 10 times the acoustic wavelength in the load medium. Hence, the minimum aperture size is 0.75 mm in length and width for a square aperture. The beam pattern was studied using Field II by varying dimensions of the aperture. Also for this transducer, the aperture size was made approximately 17 times larger than the wavelength in water, resulting in a narrow beam with shape similar to that from the mid-frequency transducer.

Two different piezoelectric materials were used for the active element in the high frequency transducers; Single crystal PMN-33PT (H.C. Materials Corp. Urbana, IL) and PZT-5H (Morgan Technical Ceramics. Stourport, England). PMN-PT single crystal was chosen for its superior electromechanical coupling coefficient, high piezoelectric constant and low dielectric loss, making it a preferable material for designing high bandwidth and

17

high sensitivity transducers. This material does however have a low coercive field and Curie temperature, meaning the material can be depoled at lower electric field strength and temperature. PZT-5H has a high electromechanical coupling coefficient. This material has a higher coercive field and Curie temperature, making the material more difficult to depole.

The standard fabrication procedure in this lab was to employ two matching layers, conductive silver epoxy for the first matching layer and parylene for the second. Conductive silver epoxy is a mix of two-component epoxy mixed with 2-3µm silver particles. This was a good choice of material in order to make electrical connections the active element. The parylene was sputtered over the whole transducer and housing. This also served as isolation for the transducers.

In the back of the piezoelectric element, a conductive backing material was used. E-solder has high attenuation, 120 dB/mm at 30 MHz, and relatively low acoustic impedance of 5.92 MRayl. This allows for low insertion loss and well-shaped pulses [20]. In addition, the backing layer provides mechanical support for the fragile active element.

Two different designs were approached. The first design, see Figure 3.4 was a transducer with two matching layers and a low impedance conductive backing material, housed in a stainless steel tubing. This was the standard fabrication technique for the ultrasound group. The drawback of this approach was the total thickness of the transducer in housing would be relatively thick. The piezoelectric element would be mounted in a 45-degree angle, relative to the housing.
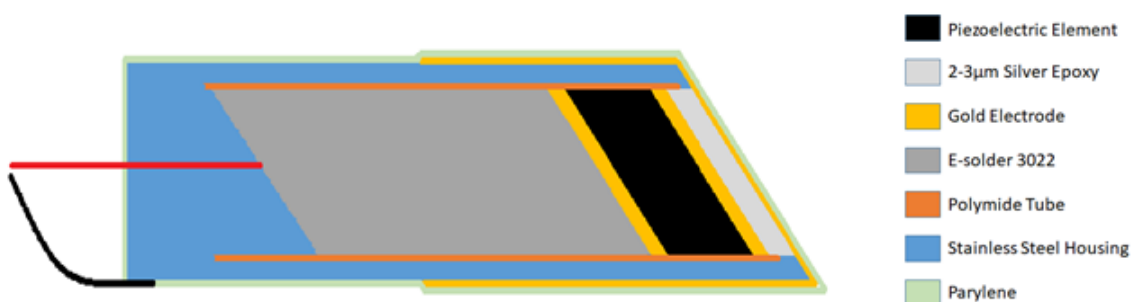
Figure 3.4 – Illustration of high-frequency transducer needle. The Piezoelectric Element (black) is Mounted in a 45-Degree Angle.

18

A second design was approached in order to reduce the total thickness of the stack, see Figure 3.5. The transducer would have a copper sheet bonded to the back of the piezoelectric element and two matching layers on top. Electrical connections would be made by connecting wires to the conductive matching layer and the copper sheet before depositing the second matching layer. This design would result in a relatively thinner stack where the piezoelectric element would be side-facing.
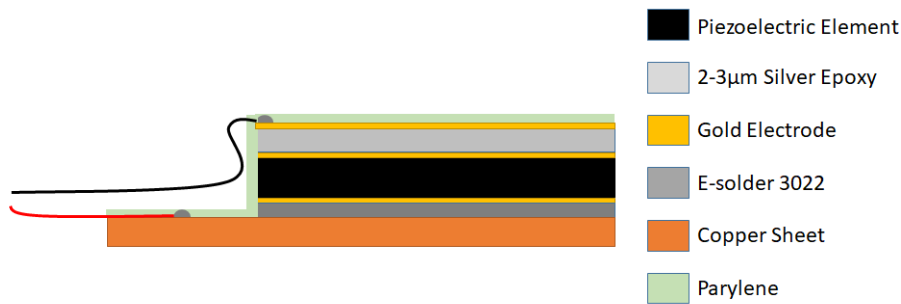
Figure 3.5 – Illustration of high-frequency "Copper Sheet" transducer.

3.2.2 Fabrication of High-Frequency "Needle" Transducers

The procedure for developing high frequency transducers is of interest for the HSN ultrasound group. One of the objectives for the thesis was to provide detailed information on the fabrication procedure. Readers are referred to Appendix B for a step-wise description of the fabrication procedure.

Two different piezoelectric materials were used for the active element in the high frequency transducers; Single crystal PMN-33PT (H.C. Materials Corp. Urbana, IL) and PZT-5H (Morgan Technical Ceramics. Stourport, England). The piezoelectric element was first lapped to an even surface before a seed layer of chrome and a gold electrode was sputtered on the element. The opposite side of the piezoelectric element was lapped to the desired thickness before a second electrode was sputtered in the same way. A matching layer of Insulcast 50 and Insulcure 9 (American Safety Technologies. Roseland, NJ) and 2-3 µm silver particles (Sigma-Aldrich Inc. St Louis, MO) was cured over the PMN-PT and lapped to the desired thickness. A conductive backing material, E-solder 3022 was cured over the opposite side of the piezoelectric element to form the backing layer. This layer was then lapped to the desired thickness. Plugs were diced out at where the aperture was 1.2 mm * 1.2 mm with a 45 degree angle. The plugs were placed inside a polymide tube and a coaxial cable was connected with E-solder 3022 to the conductive backing. The

plugs inside the polymide tube were housed in a stainless steel needle and secured with Epotek 301 (Epoxy Technology Inc. Billerica, MA). The shield wire of the coaxial cable was connected to the needle housing using E-solder 3022. An electrode was sputtered across the silver matching layer and the needle housing to form the ground connection. Vapor deposited parylene was used to coat the aperture and the needle housing. At last, the coaxial cable were connected to a 1/4" SMA adapter with conductive silver epoxy.

3.2.3   Fabrication of High-Frequency "Copper Sheet" Transducers

For a complete and detailed description of the fabrication steps, readers are referred to Appendix C.

Two different piezoelectric materials were used for the active element in the high frequency transducers; Single crystal PMN-33PT (H.C. Materials Corp. Urbana, IL) and PZT-5H (Morgan Technical Ceramics. Stourport, England). The piezoelectric element was first lapped to an even surface before a seed layer of chrome and a gold electrode was sputtered on the element. The opposite side of the piezoelectric element was lapped to the desired thickness before a second electrode was sputtered in the same way. A matching layer of Insulcast 50 and Insulcure 9 (American Safety Technologies. Roseland, NJ) and 2-3 µm silver particles (Sigma-Aldrich Inc. St Louis, MO) was cured over the PMN-PT and lapped to the desired thickness. The piezoelectric element with a conductive matching layer were bonded to a copper sheet using conductive epoxy E-solder 3022 (VonRoll, Isola. New Haven, CT). A coxial cable was connected with E-solder 3022 to the conductive matching layer, the shielding wire was connected to the copper sheet. Vapor deposited parylene was used to coat the matching layer, wires and the copper sheet. 1.2 mm * 1.2 mm transducer elements were diced out from the larger sample.

3.3   Modelling of Piezoelectric Ultrasound Transducer

The following subchapter gives an overview of the methods used to simulate the fabricated transducers. First, a description of the one-dimensional model is given, followed by a detailed overview of the finite element model. Finally, simulations to model the beam profile in Field II are explained. All material parameters used for the simulations are listed in 4.1.

3.3.1 One Dimensional Model of Ultrasound Transducer

Xtrans was used to evaluate the performance of all fabricated transducers. Material parameters to describe each layer of the transducer is input to a user interface. PiezoCAD was briefly used in the USC Biomedical Lab to predict the performance of the high frequency transducers prior to fabrication. Material parameters used for the one-dimensional Mason model are listed in 4.1.1.

A simple comparison of a high frequency transducer using the Mason model and KLM model was performed in order to evaluate the resemblance of the two models.

3.3.2 General Description of FEM Model

A finite element model of the mid- and high-frequency transducers was made using COMSOL. Material parameters are listed in Table 4.1.2. A description of the steps taken to model the transducers follows.

Geometry: The model was built using the included CAD features in COMSOL. Rectangles to represent the perfectly matched layer, load and transducer stack was built. The geometry was kept as a layer sequence of a single block to make it easier to make changes to layer dimensions. *Perfectly Matched Layer* was defined for the domain highlighted in cyan in Figure 3.6. The perfectly matched layer simulates the zero reflection condition, i.e. this layer absorbs outgoing waves without reflecting the waves back to the transducer surface. The blue domain of Figure 3.6 is the load and red is the transducer stack.
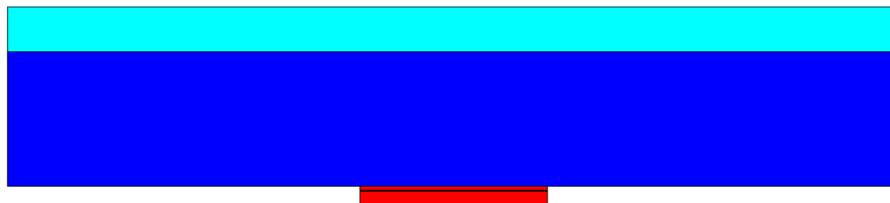
Figure 3.6 – General description of the whole model. Transducer stack in red is small compared to load in blue and perfectly matched layer in cyan.

Figure 3.7 shows the mid-frequency transducer stack (left) and high-frequency transducer stack (right).

Figure 3.7 – Enlarged section of COMSOL model of the mid-frequency transducer (left) and high-frequency transducer (right). Mid-frequency transducer is modeled with piezoelectric element (red domain) with electrodes on both sides, a bond line (not visible) and a matching layer. High frequency transducer is modeled with a piezoelectric element with electrodes on both sides, two matching layers and a backing layer.

Materials: Some materials needed for the model are readily available, however most are not. Air and water was used for the load in the simulations and were readily available in the library. Silver and gold for the electrodes and piezoelectric material PZT5-H were also available in the library. The materials that were not included in the library and had to be added were the following: Piezoelectric materials PZ29 and PMN-33PT. Matching layer materials 2-3 silver epoxy, parylene, Eccosorb MF114 and Eccosorb MF1112. Bonding layer material 3M DP460 adhesive epoxy. Backing layer material Esolder 3022.

Physics: *Pressure Acoustics* physics was chosen for domains highlighted in blue and cyan of Figure 3.8. Temperature and absolute pressure was set as room temperature and one atmosphere, respectively. Yellow line of Figure 3.8 was set as *Sound Hard Boundary*, which sets the normal acceleration on the boundary to zero, emulating a wall.
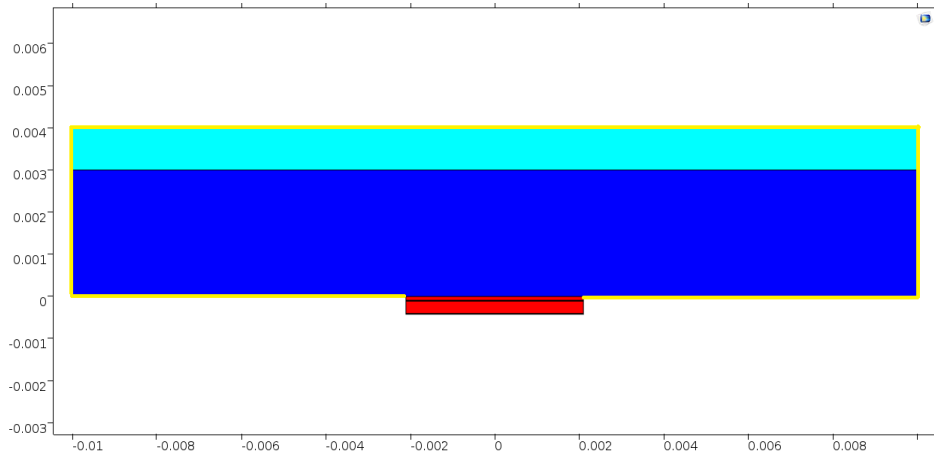
Figure 3.8 – *Pressure Acoustics* **added to domains in blue and cyan. Yellow line is defined as** *Sound Hard Boundary.*

Solid Mechanics was applied to the transducer shown in Figure 3.9. The domains highlighted in green are set as linear elastic while the red section of the transducer is *Piezoelectric*. The blue line surrounding the transducer has the boundary condition *Free*, which defines the boundaries as free to move in any direction.
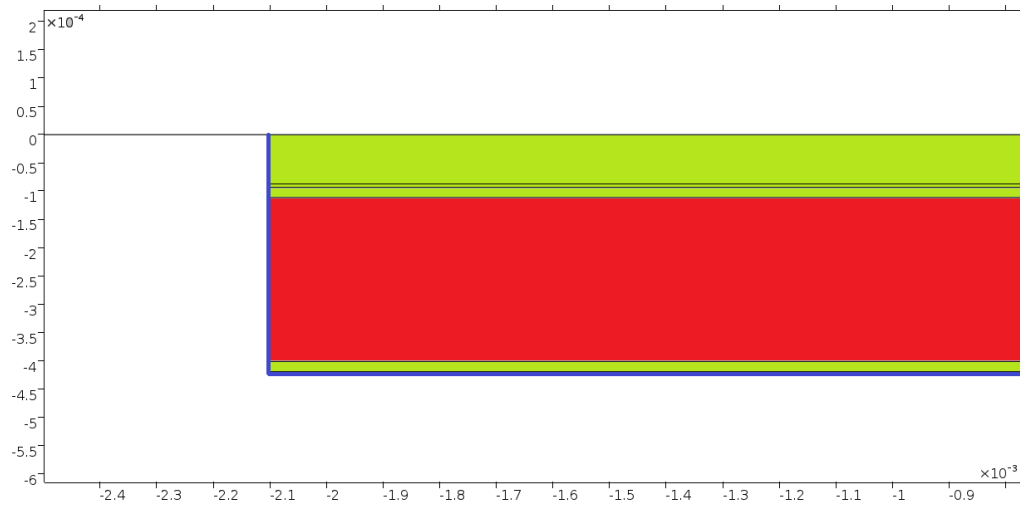
Figure 3.9 – *Solid Mechanics* **applied to the modeled transducer. Red domain is defined as** *Piezoelectric*, **green is defined as** *Linear Elastic*. **Blue line sets the boundary condition** *Free*

Electrostatics was added to the area highlighted in light blue of Figure 3.10. The red lines indicate the boundary conditions *Ground* and *Electric Potential*, applied to the top and bottom boundary of the piezoelectric material, respectively. The yellow line indicates the boundary condition *Free Charge*, which defines that there is no electric charge on the boundary.

23
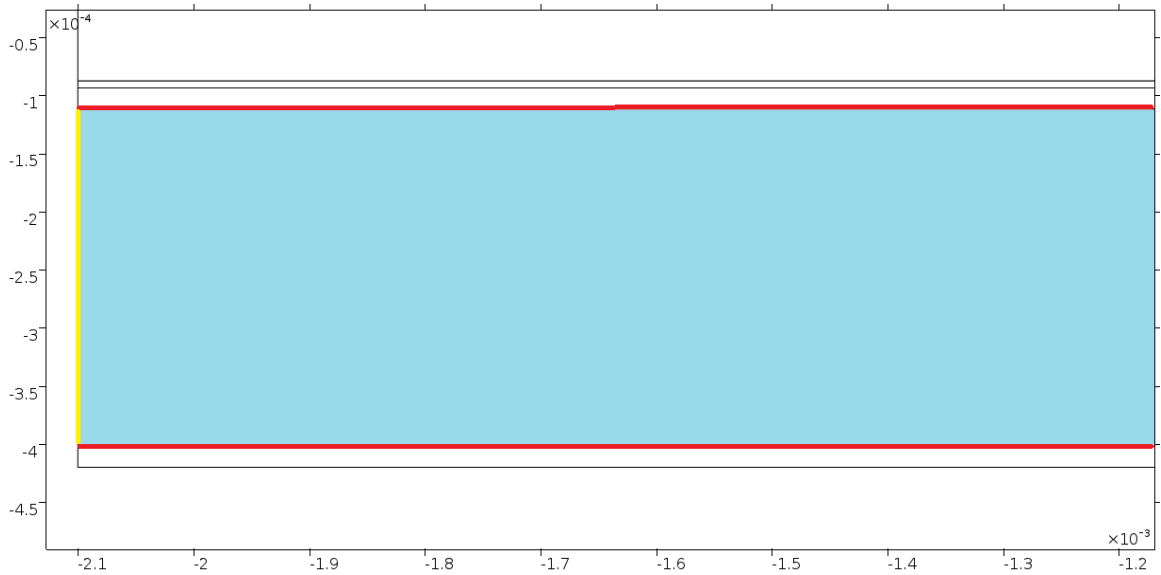
Figure 3.10 – *Electrostatics* **applied to the light blue domain. Red line on top and bottom is** *Ground* **and** *Electric Potential***, respectively. Yellow line on the side is defined as** *Free Charge***.**

The *Multiphysics* options were used to couple the interfaces between different physics modules. *Piezoelectric Effect* couples *Solid Mechanics* to *Electrostatics*. An *Acoustic-Structure Boundary* was set at the interface between the matching layer and the load which couples the *Pressure Acoustics* to the *Solid Mechanics*.

Mesh and element size: Free Triangular mesh was selected for all domains where the element size was set as Finer, giving a dense mesh. The models were studied in frequency domain by performing a frequency sweep with a frequency step size of 50 kHz.

Post processing: Data was extracted from the simulated models by evaluating a line integral to a set of equations defined under Definitions. The integral operation is used to obtain the integral value of the current density over the width of the piezoelectric. The integral operation was done by adding a component coupling to the boundary of the top electrode of the piezoelectric element. The impedance magnitude and phase was calculated from the following equations:

$$I^{PZT} = -l \int_0^w j_y \, dx \qquad\qquad (3\text{-}1)$$

$$Z^{PZT} = \frac{V^{PZT}}{I^{PZT}} \qquad\qquad (3\text{-}2)$$

Equation 3.1 is the integral over the width to give the electrical current flowing in the piezoelectric element. j_y is the current density along the y-direction. l and w are the length and width of the element respectively. The negative sign is due to the polarization of the piezoelectric element. Equation 3.2 is the electrical impedance of the element where V^{PZT} is the voltage applied over the two electrodes, defined in the parameter list as 1V. The impedance phase is given by the argument function operation on the complex values of Z^{PZT}. All data were exported from COMSOL to MATLAB for comparison with Mason model and measurements.

Losses: In order to model the piezoelectric material as accurately as possible, losses have to be considered. The three following paragraphs describe how the loss was defined for PZT-5H, PMN-PT and PZ29, respectively.

Two similar datasets were used to model the PZT-5H in FEM. The first dataset was taken from the COMSOL Library for piezoelectric materials, and the second dataset was provided from the USC group. The loss for the piezoelectric material was defined as isotropic, using only the mechanical loss factor Q_m.

Zhang et. al. [22] has provided sufficient material parameters to model PMT-PT using FEM. The material described in literature is a PMN-33PT, poled along the [001] axis. The actual material in the fabricated transducer is PMN-33PT and the element is assumed to be poled along the [001] direction. The loss for the piezoelectric material was defined as isotropic, using only the mechanical loss factor Q_m.

Material data from Ferroperm was used to describe PZ29. Two methods to account for the loss were approached. Aanes et. al. [23] calculated a new set of constants for PZ27, a similar material to PZ29, by applying Sherrit's Method [24] and then adjusting the values to fit measurements. The constants are described by a full set of complex values that account for the dielectric, elastic and piezoelectric losses. The imaginary part of these complex constants, which represent the losses, was used in the FEM simulations to

describe PZ29. A second approach to account for the losses was to use a simplified model where the mechanical loss was described by the loss factor Q_m.

3.3.3 Modeling of Beam Profile

Field II (version 3.20) was used to simulate the beam profile of the transducers. Various aperture sizes were tested for the 6MHz and 20 MHz transducer in order to find the optimal beam shape.

The excitation of the transducer consisted of two periods of a sinusoid dependent on the center frequency. The impulse response of the aperture was a two-cycle sinusoid, center frequency dependent, Hanning weighted pulse. The parameters used to define the mid-frequency and high-frequency transducers are listed in Table 4.1.3.

3.4 Characterization of High- and Mid-Frequency Transducers

The transducers were characterized in the HSN ultrasound lab. Electrical impedance measurements were performed following each step of the mid-frequency transducer fabrication to study the effect of adding matching layers and electrical connections. The beam profile of selected high frequency needle transducers was measured. Pulse echo measurement were performed on selected mid-frequency transducers.

3.4.1 Electrical Impedance Measurements

Electrical impedance measurements on the fabricated transducers were performed using network analyzer HP 8753D (Agilent Technologies Inc. Philadelphia, PA). Measurements were acquired in LabVIEW (National Instruments Corp. Austin, TX) and imported to MATLAB for analysis and plotting.

Most of the measurements were performed using air as load. This was done since the resonance peaks are more apparent than in water. Measurements in water were performed on selected mid-frequency transducers prior to pulse echo measurements by submerging the transducers in a beaker filled with water.

To measure mid-frequency transducers, the network analyzer was calibrated for a needle probe, as shown in Figure 3.11, in the frequency range 30 kHz-20 MHz with 1601 data points. The calibration was done in open, short and 50Ω termination of the probe.

Figure 3.11 – Electrical impedance measurement setup for characterizing mid-frequency transducers. The network analyzer was calibrated for the needle probe shown in the figure. The figure demonstrates how the piezoelectric element alone was measured. The copper chuck was also calibrated for in this case.

To measure the electrical impedance of the high frequency transducers, the network analyzer was calibrated by connecting an SMA adapter directly in the Port 1 of the network analyzer, as shown in Figure 3.12. The calibration was done for frequency range 30 kHz-40 MHz with 801 data points.
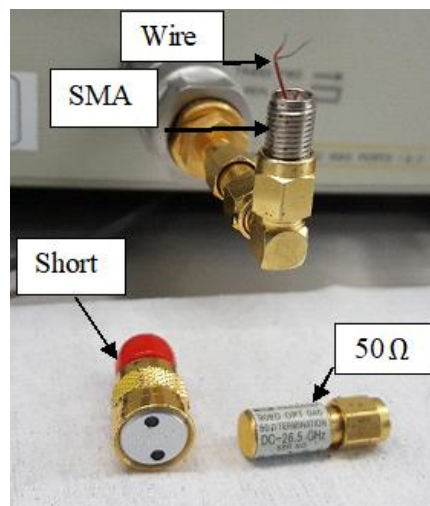
Figure 3.12 – Calibration of network analyzer for measurements on high-frequency transducer. SMA adapter is calibrated in open, short and 50Ω termination. The wire shown in the figure was not part of the calibration, but was later measured to study its influence on impedance measurements of the high frequency transducers.

3.4.2 Poling of PMN-PT Needle Transducers

Electrical impedance measurement on the PMN-PT transducers indicated an error, as no resonances were observed in the fabricated transducers. An attempt at poling the piezoelectric elements was conducted. 237-High Voltage Source Unit (Keithley Instruments. Cleveland, OH) was used to sweep a DC 80V amplitude waveform, as shown in Figure 3.13. The transducer was connected to the voltage source in series with a 1kΩ

current limiting resistor. After the voltage sweep, the circuit was shorted to discharge the transducer. Figure 3.14 shows the setup used for poling the transducers.
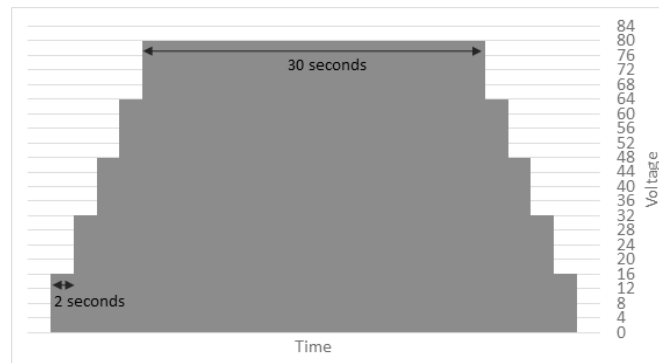
Figure 3.13 – High voltage waveform used to pole PMN-PT transducers. The waveform had an amplitude of 80V.
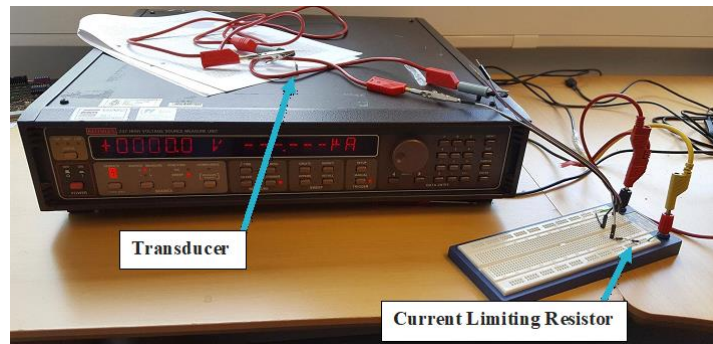
Figure 3.14 – Setup for poling PMN-PT transducers. The transducer was connected to the voltage source in series with a 1kΩ current limiting resistor.

3.4.3 Beam Profile Measurement

Panametrics Pulser Reciever 5052PR(Olympus Corp. Waltham, MA) was used to drive the high frequency transducers during the measurement. This pulser generates a voltage pulse of short duration, assumed to represent an impulse, or Dirac Delta function. Due to the high output voltage, it was not possible to measure this pulse with our available equipment.

The LeCroy LT342L oscilloscope (LeCroy Corp. Chestnut Ridge, NY) monitored pulses from the waveform generator. Sound pulses were measured using an Onda HGL-0200 hydrophone (Onda Corp. Sunnyvale, CA) by scanning laterally, normal to the acoustic axis at a fixed distance and in a plane along the acoustic axis. The Onda AIMS II

software determined the orientation of the plane. The calibration of the Onda hydrophone is valid in the frequency range 1 MHz-20MHz.

The output of the hydrophone at each position was digitized at 250 MSa/s in the Picoscope PS5244A analog to digital converter(Pico Technology. St Neots, UK). The received pulses were transferred to a computer to be stored and analyzed in Matlab.

3.4.4   Pulse Echo Measurement

The transmit transfer function, $H_{tt}(f) = U(f)/V(f)$, was measured for selected mid-frequency transducers using the pulse echo set up [25]. H_{tt} was calculated according to [17]. The electrical chain was compensated for by calculating the influence of the electrical wires in Matlab. There were no correction for attenuation or for diffraction since we assumed plane waves.

The transducer was mounted in a tank of de-ionized water. The transducer was connected to a 50Ω signal generator NI PCI-5412 (National Instruments Corp. Austin, TX) and excited with a sine wave of two periods weighted with a Hanning window. 4V amplitude and center frequency of 6 MHz was used for the excitation pulse. A polished brass disc with a reflection coefficient of 0.92, was used to the reflect the transmitted pulse. The received signals were recorded by the NI PCI-5122 oscilloscope (National Instruments Corp. Austin, TX) in LabView and processed in Matlab.

4 Results

This chapter is organized as follows: Section 4.1 lists the material parameters and input parameters used for simulations. 4.2 describes the result of fabricating mid-frequency single element transducers. The fabricated transducers are studied and characterized by electrical impedance measurements and pulse-echo measurements. Section 4.3 describes the result of fabricating high-frequency needle transducers. The transducers are characterized by electrical impedance measurement and by beam profile measurements. Section 4.4 describes the fabrication results of the "copper sheet" transducers.

4.1 Material Parameters

For ease of comparing material parameters to graphs, the material parameters used for all theoretical models are listed in this section. First, active and passive material parameters for the one-dimensional mason model are given. Next, several datasets for the finite element simulations are presented. Then an overview is given for the input parameters for the Field II simulations.

4.1.1 One-dimensional Mason Model

Table 4.1 lists the material parameters for the piezoelectric element used in the one-dimensional Mason model. PZ29 was used for the mid-frequency transducers. PMN-33PT and PZT-5H was used for the high-frequency transducers.

Table 4.1 –Active Materials used for Mason Model

	Piezoelectric Constant H_{33} [V/m]	Relative Permittivity $\varepsilon_{33}^{s}/\varepsilon_0$	Acoustic Impedance Z [MRayl]	Longitudinal Velocity v_l [m/s]	Mechanical Loss Factor Q_m [-]
			PZ29		
From supplier[AD]	19.6	1220	33.56	4498.24	195
Fitted	16.5	-	-	-	80
			PZT5-H		
From Literature	18.31 [C]	1704 [C]	34.20 [C]	4560 [C]	65 [26]
			PMN-PT		
From Literature	33.7 [22]	797 [27]	36.90 [27]	4608 [27]	69 [26]

[#] – Reference
[C] – COMSOL data
[AD] – Reference to Appendix D

Table 4.2 lists the material parameters for the load medium as well as the passive materials used in the one-dimensional Mason model of the mid- and high-frequency transducers.

Table 4.2 – Passive Materials Used For Mason Model

	Acoustic Impedance Z [MRayl]	Longitudinal Velocity vl [m/s]	Mechanical Loss Factor Qm [-]
Acoustic Properties of Load			
Air 20° C	0.000413 [31]	343 [31]	10 [-]
Water 20° C	1.48 [32]	1480 [32]	10 [-]
Acoustic Properties of Passive Materials for Mid Frequency Transducer			
Eccosorb MF114 [29]	6.51	2246	38
Fitted Eccosorb MF114	-	-	20
Eccosorb MF112 [29]	4.94	2389	39.624
3M Adhesive Epoxy [29]	2.8	2450	12.5
Silver Electrode	37.8 [30]	3600 [30]	10 [-]
Acoustic Properties of Passive Materials for High Frequency Transducer			
2-3 Silver Epoxy	7.3 [28]	1900 [28]	32.07 [28]
Parylene	2.60 [28]	2200 [28]	41 [USC]
Esolder 3022	5.92 [28]	1850 [28]	4.02 [28]
Gold Electrode	62.6 [30]	3240 [30]	10 [-]

[#] – Reference
[USC] – Characterized by USC ultrasound group
[-] – Mechanical loss factor of electrodes and loads are assumed 10 as these have minimal influence

4.1.2 FEM Model

Table 4.3 lists the material parameters for the piezoelectric materials used for the finite element simulations.

Table 4.3 – Active Materials Used For FEM Model

		PZ29 [23]	PZT5-H [C]	PZT5-H [USC]	PMN-PT [22]
Elasticity Matrix $[10^{11}\,\text{Pa}]$	C_{11}	1.34(1+i/110)	1.27205	1.272	1.15
	C_{12}	0.897(1+i/250)	0.802122	0.802	1.03
	C_{13}	0.857(1+i/200)	0.846702	0.847	1.02
	C_{22}	1.296(1+i/110)	1.27205	1.272	1.15
	C_{33}	1.09(1+i/177.99)	1.17436	1.174	1.03
	C_{44}	0.185(1+i/75)	0.229885	0.23	0.69
	C_{55}	0.185(1+i/75)	0.229885	0.23	0.69
	C_{66}	0.220(1+i/75)	0.234742	0.235	0.66
Coupling Matrix $[\text{C/m}^2]$	E_{15}	13.40(1-i/200)	17.0345	17	10.1
	E_{24}	13.40(1-i/200)	17.0345	17	10.1
	E_{31}	-5.06(1-i/70)	-6.62281	-6.5	-3.9
	E_{32}	-5.06(1-i/70)	-6.62281	-65	-3.9
	E_{33}	21.2(1-i/200)	23.2403	23.3	20.3
Relative Permittivity	ε_{11}	1340(1-i/50)	1704.4	1700	1434
	ε_{22}	1340(1-i/50)	1704.4	1700	1434
	ε_{33}	1221.63(1-i/80)	1433.6	1470	680
Density $[\text{kg/m}^3]$	ρ	7460	7500	7500	8060
Longitudinal Speed [m/s]	v_l	4498.24	4560	4560	4610
Mechanical Loss	Q_m	195	65[26]	65	69 [26]

[#] – Reference
[USC] – Characterized by USC ultrasound group
[C] – COMSOL data

Table 4.4 lists the material parameters for the piezoelectric elements used for the finite element simulations. Shear velocity for passive materials used in high frequency transducer was obtained from USC's PiezoCAD database. E-solder 3022, used for the backing layer, is described with a complex value to account for the loss in the material.

Table 4.4 – Passive Materials Used For FEM Model

	Density ρ [kg/m^3]	Longitudinal Velocity vl [m/s]	Shear Velocity vs [m/s]
Acoustic Properties of Passive Materials for Mid Frequency Transducer			
Eccosorb MF114 [29]	2900	2246*(1+i*0.018)	1145*(1+i*0.032)
Eccosorb MF112 [29]	2066	2389*(1+i*0.018)	1170*(1+i*0.032)
3M Adhesive Epoxy [29]	1200	2500*(1+i*0.029)	1180*(1+i*0.05)
Acoustic Properties of Passive Materials for High Frequency Transducer			
2-3 Silver Epoxy [28]	3860	1900	1343
Parylene [28]	1100	2350	1661.7
Esolder 3022 [28]	3200	1850(1+i0.25)	1146(1+i0.50)

[#] – Reference

4.1.3 Field II

Table 4.5 lists the input parameters used to the define the transducer aperture in Field II.

Table 4.5 – Field II Parameters

Parameter	High Frequency Transducer
Sample Rate	500 MHz
Center Frequency	20 MHz
Bandwidth	50%
Speed of Sound	1540 m/s
Excitation Pulse Length	200 ns
Number of Elements	1
Element Width (Azimuth)	1.2 mm
Element Height (Elevation)	1.2 mm

4.2   Mid-Frequency Single Element Transducers

4.2.1   Fabricated Mid-Frequency Transducer

Build specifications of the fabricated transducers are summarized in Table 4.6.

Table 4.7 describes each fabricated transducer and names are given for referencing.

Table 4.6 – Mid-Frequency Transducer Build Specifications

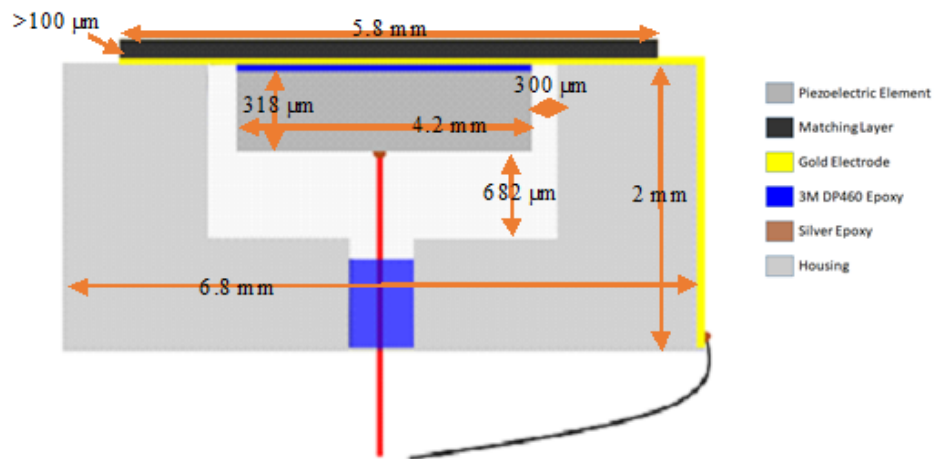|	MF114	MF112
Yield	6 transducers	1 transducer
Housing	3D printed plastic housing sputtered with gold. 3D printed probe for acoustic measurements. See Figure 4.1 for dimensions	
Connections	Copper wire	
Piezoelectric Element	PZ29 (Ferroperm A/S) with silver painted electrodes on top and bottom of element. Active element thickness: 296 µm ± 1 µm Top electrode thickness: 10 µm ± 2 µm Bottom electrode thickness: 10 µm ± 2 µm Length: 4.2 mm Width: 4.2 mm	
Matching layer Thickness	85-96 µm	98 µm
Matching layer Area	Length: 5.8 mm Width: 5.8 mm	
Bonding layer	3M DP460 Epoxy Thickness: 3 µm	
Sputtered electrode thickness on matching layer and housing	Chrome: 25 nm (seed layer) Gold: 150 nm	
Backing layer	Air	

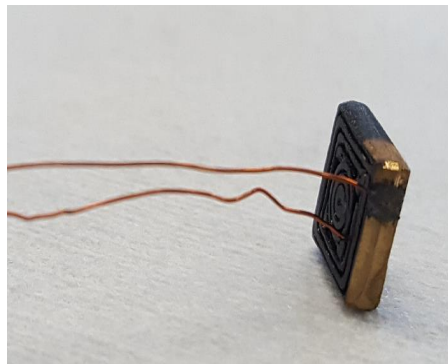**Figure 4.1 – Layers and Dimensions of Mid Frequency Transducer. Figure is not drawn to scale.**

Figure 4.2 – Fabricated Mid Frequency Transducer in Housing with Wires Connected

Table 4.7 – Overview of Fabricated Mid-Frequency Transducers

Transducer Reference Name	Matching layer Material	Matching layer thickness	Bonding layer Thickness	PZ29 thickness
Stack 1	Eccosorb MF114	96 µm ± 2 µm	3 µm	318 µm ± 0.5 µm
Stack 2	Eccosorb MF114	96 µm ± 2 µm	3 µm	318 µm ± 0.5 µm
Lapped Stack 2	Eccosorb MF114	85 µm +- 3 µm	3 µm	318 µm ± 0.5 µm
Stack 3	Eccosorb MF114	96 µm ±1 µm	3 µm	318 µm ± 0.5 µm
Stack 4	Eccosorb MF112	98 µm ±1 µm	3 µm	318 µm ± 0.5 µm
Stack 5	Eccosorb MF114	94 µm ± 3µm	8 µm ± 5 µm	318 µm ± 0.5 µm
Stack 6	Eccosorb MF114	95 µm ± 5µm	8 µm ± 4 µm	318 µm ± 0.5 µm
Stack 7	Eccosorb MF114	94 µm ± 6µm	6 µm ± 3 µm	318 µm ± 0.5 µm

4.2.2 Preliminary Study of Material Parameters

As described in section 3.1.3, a fabricated transducer was compared to the theoretical model to study the accuracy of the material parameters. Material parameters for PZ29 and Eccosorb MF114 were fitted to match the measured results.

Figure 4.3 shows the electrical impedance measurement of five square samples of PZ29 with dimensions 4.2 mm * 4.2 mm. Sample 1,3 and 5 measured 318 µm ± 0.5 µm, and Sample 2 and 4 measured 330µm ± 2 µm. Sample 2 and 4 indicate a lower resonant frequency than the three other samples. This is as expected as the resonance frequency is dependent on the thickness of the piezoelectric material, as described in Equation 2-2.
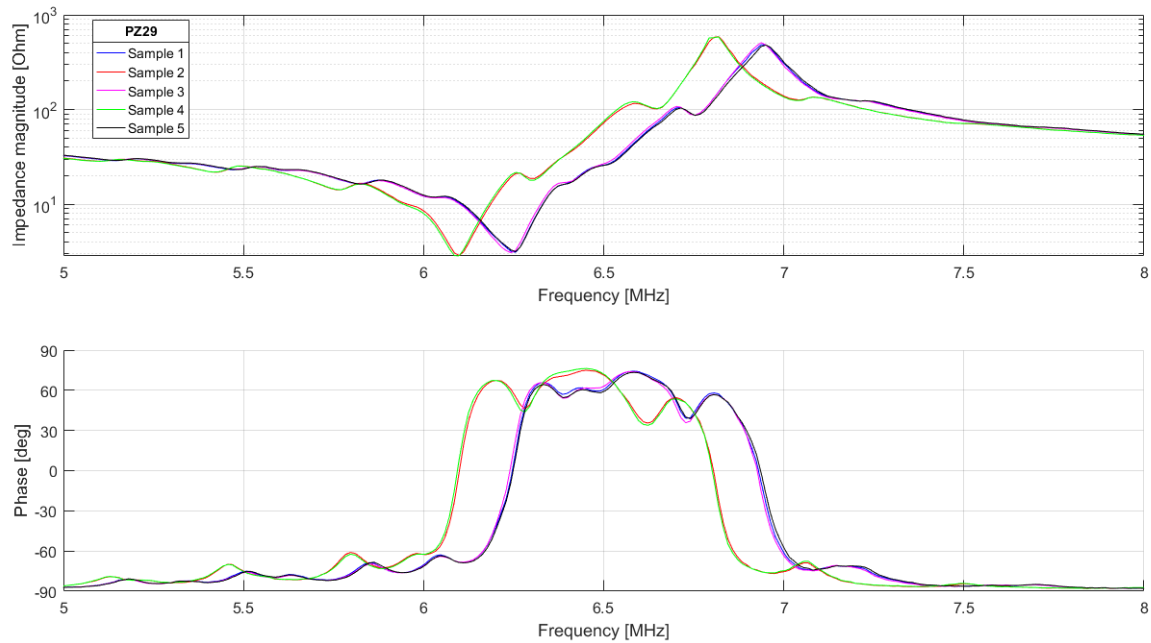

Figure 4.3 – Electrical Impedance Measurement on 5 square samples of PZ29 with length and width of 4.2 mm. Measured thickness of sample 2 and Sample 4 was 330 µm. Measured thickness of Samples 1, 3 and 5 was 318 µm.

Figure 4.4 shows the electrode thickness for three different samples. The image is obtained from optical microscopy with 1000X magnification. The electrode thickness was found to be 10µm ± 2µm.

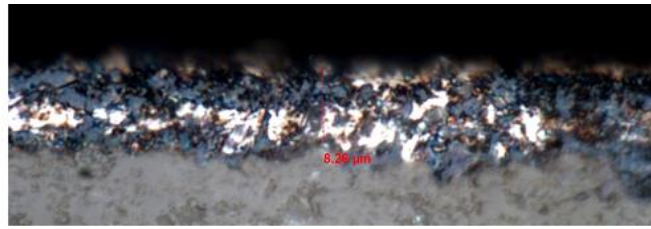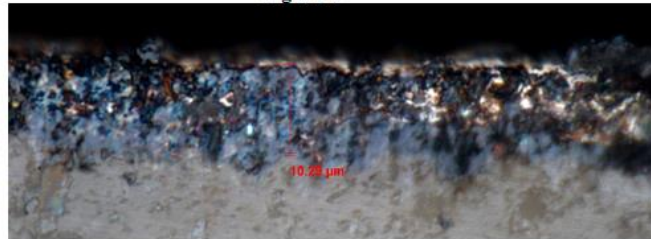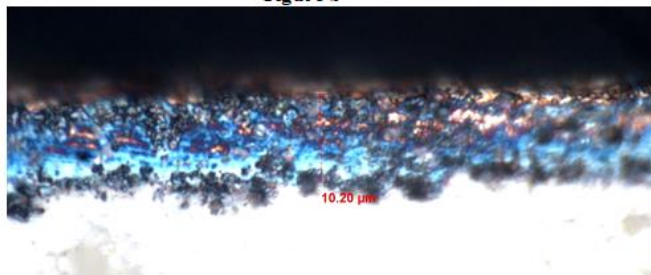**Figure 4.4 - Optical Microscope Image of PZ29 Electrode Thickness. Thicknesses measured are; A=8.26μm, B=10.29μm, C=10.20μm.**

Figure 4.5 shows the measured electrical impedance of one of the samples with thickness 318 μm in red along with the one-dimensional Mason model. The pink dashed line is the material data from the manufacturer, Ferroperm. The measured resonance peak is not as sharp as predicted from the Mason model, indicating that the damping is higher than given by the material data, i.e. the Q-factor is lower than the Q-value from the manufacturer. The green stippled line is the fitted Q value. The distance between anti-resonance and resonance is too high, indicating that the coupling factor H_{33} is overestimated. The mechanical Q-factor and H_{33} value was fitted, resulting the blue line. The fitted material parameters for PZ29 are listed in Table 4.1 –Active Materials used for Mason Model.
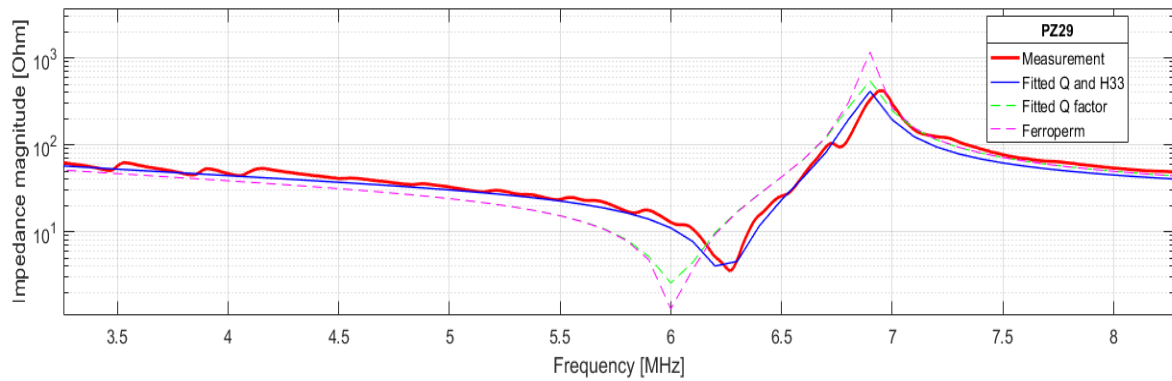
Figure 4.5 – Process of fitting material parameters for PZ29 in Mason model. The red line is the measured electrical impedance. The pink dashed line is the result from Mason model using material parameters from Ferroperm. The Q factor has been reduced in the green dashed line. The blue line is the result of the fitting where the Q-factor and H_{33} have been adjusted from 195 to 80 and from 19.6 to 16.5, respectively.

The PZ29 element used for fitting the material parameters was then bonded to a matching layer to form Stack 3. As seen in Figure 4.6, The electrical impedance of Stack 3, red line, was measured and compared to the Mason model, green line. Fitted values for PZ29 and data for Eccosorb MF114 [29] and 3M DP460 Epoxy [29] were used. A slight improvement in the theoretical model was found by decreasing the Q-factor for the matching layer from 195 to 80. The material parameters for the bonding layer were kept as they were. This is a reasonable assumption, as the bonding layer is thin relative to the matching layer. Table 4.2 – Passive Materials Used For Mason Model lists the material parameters for Eccosorb MF114 and 3M DP460 epoxy, before and after fitting.
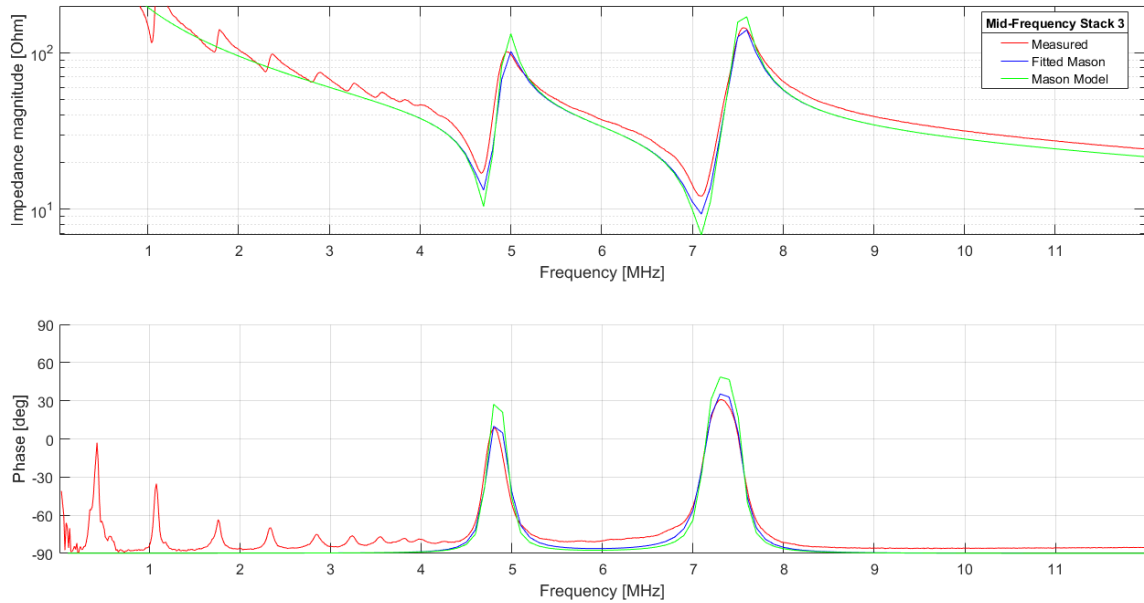
Figure 4.6 – Fitting of material parameters for Eccosorb MF114. Red line shows the measured electrical impedance of a stack consisting of PZ29 bonded with 3M DP460 Epoxy to matching layer Eccosorb MF114. Green line shows the result from Mason model. The Q-factor was adjusted from 38 to 20, shown by the blue line.

4.2.3 FEM Simulations of PZ29

FEM simulations of electrical impedance for PZ29 were performed in COMSOL, using material data from Ferroperm. Two different approaches to account for the loss in the piezoelectric were performed, as described in the last paragraph of section 3.3.2.

Figure 4.7 shows the result of the simulation, along with the one-dimensional Mason model, using material data from Ferroperm, and a measured sample. The simulation result from using isotropic loss and complex loss is shown by the red line and blue line, respectively. The result from the Mason model is shown in blue. The black dashed line shows the measured electrical impedance of a square sample of width and length 4.2 mm.
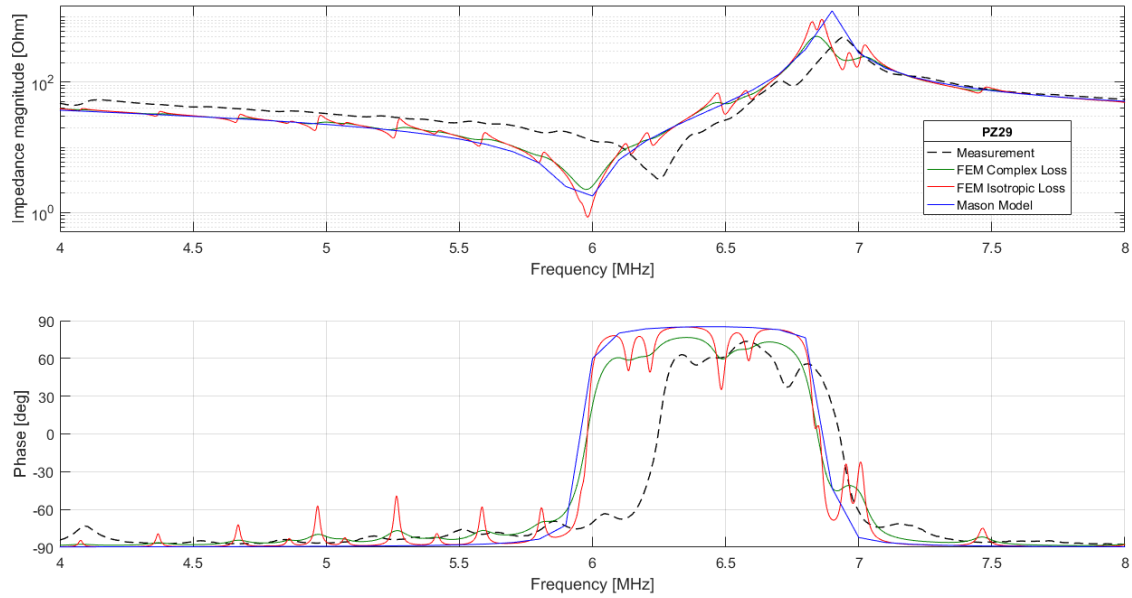
Figure 4.7 - Result of COMSOL simulation (red – isotropic loss) (green – complex loss), along with one-dimensional Mason model (blue) and a measured sample (dashed black). Material parameters from Ferroperm was used for the Mason model and the COMSOL simulations. Isotropic loss was defined by 1/195 for the piezoelectric material. Complex loss was defined by using the imaginary parts of complex values, i.e. loss values, for a similar material, Ferroperm PZ27.

4.2.4   Electrical Impedance of Stack 1-3

Mid-frequency transducer Stacks 1, 2 and 3 were fabricated close to identical. The measured electrical impedances in air are shown in Figure 4.8, with Mason model in black dashed line and COMSOL simulation in pink dashed line. Material parameters from Ferroperm with the complex loss was used in the COMSOL simulations. Fitted material parameters were used for the Mason model.
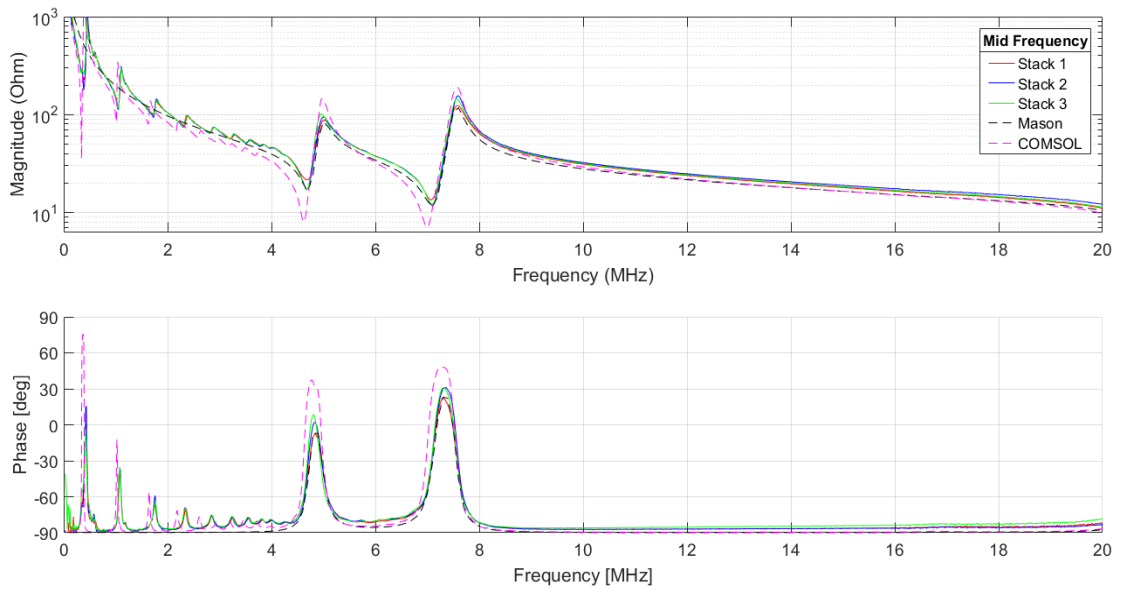
Figure 4.8 – Electrical impedance measurement in air on Stack 1 (red), Stack 2 (blue) and Stack 3 (green), before connecting wire and housing. The fabricated transducers were close to identical and electrical impedance measurement result reflected this. The Mason model, shown by black dashed line, corresponds well with measurement results. COMSOL simulations using material data from Ferroperm and complex loss, shown by pink dashed line, indicate higher impedance magnitude than what was measured.

Stacks 1-3 and were connected with a wire to the bottom electrode of the piezoelectric and housed in 3D printed housing that had been sputtered with gold. Figure 4.9 shows the electrical impedance of Stack 1 (red), Stack 2 (blue) and Stack 3 (green) with a wire and housing connected.
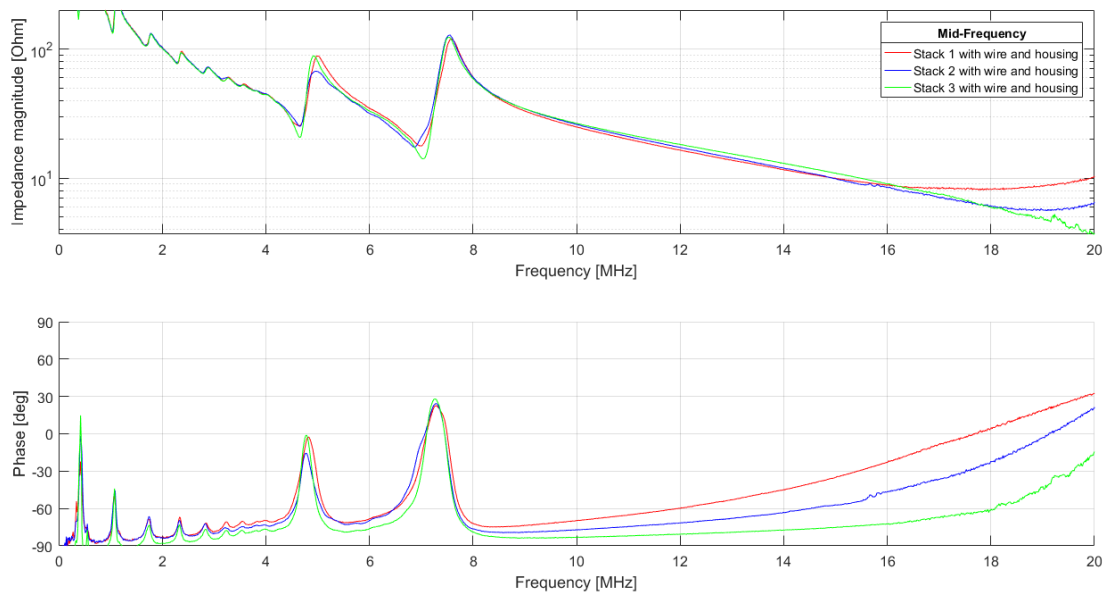

Figure 4.9 – Electrical impedance of Stack 1 (red), Stack 2 (blue) and Stack 3 (green) after connecting wire and housing. An inductance caused by the wire is observed at higher frequencies. The variation in inductance between the stacks is due to variation in wire length for each stack.

44

To study the influence of the electrical connections, the electrical impedance of Stack 3 was measured at each step; stack alone, stack with wire and stack with wire and housing. Prior to connecting, the impedance of the wire and housing was measured. Figure 4.10 shows the influence of electrical connections on Stack 3. The influence of the electrical connections were compensated for in Figure 4.11, by subtracting the measured impedance of the wire and housing in MATLAB.
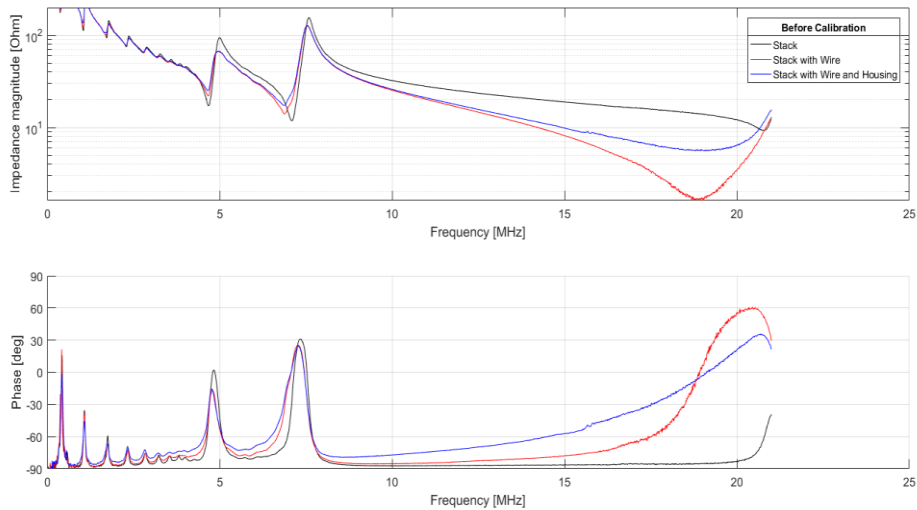

Figure 4.10 – Electrical impedance measurement of Stack 3 in black, Stack 3 with wire connected in blue, Stack 3 with wire and housing in red.
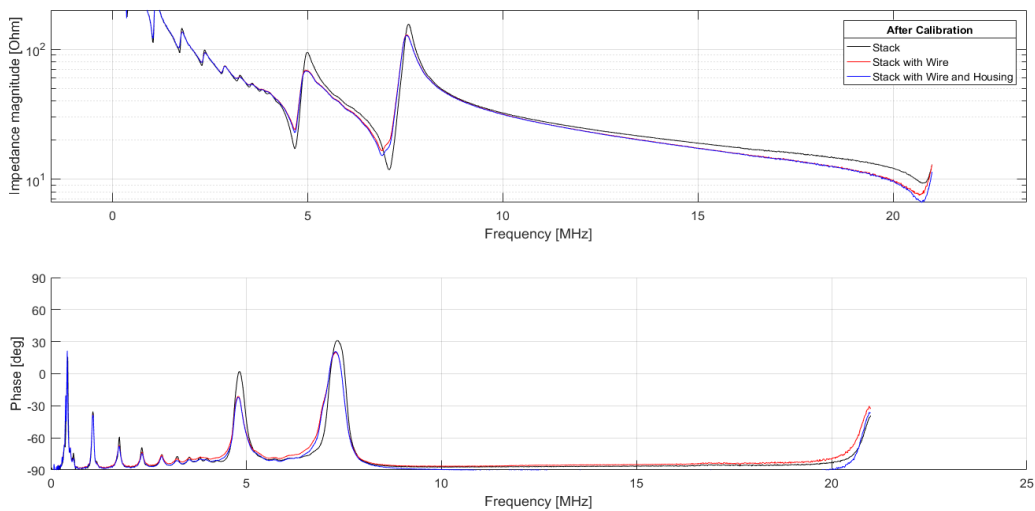

Figure 4.11 – Electrical impedance measurement on Stack 3 where the influence of wire and housing have been compensated for.

The achieved thickness of the matching layer was 96 µm, which was slightly higher than the desired thickness of 85 µm. The matching layer of Stack 2 was reduced slightly by lapping the matching layer after the transducer was connected to the housing. Figure 4.12 shows the result before and after lapping.
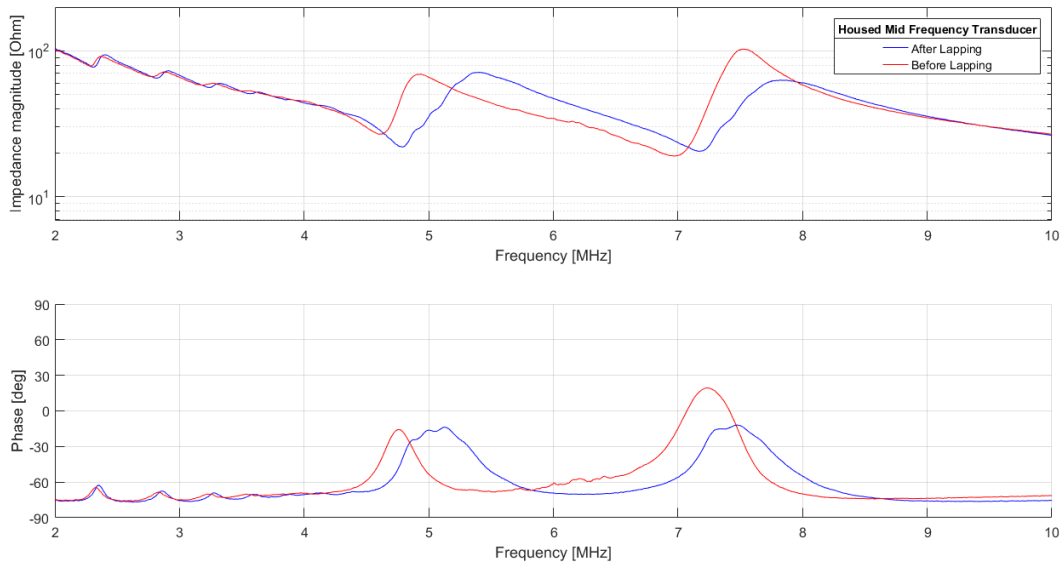
Figure 4.12 – Electrical impedance measurement on Stack 2 before and after lapping, shown in blue and red, respectively. The matching layer was lapped after packaging the stack in a housing. The thickness before and after lapping were 96 µm and 85µm, respectively.

4.2.5   Electrical Impedance of Stack 4

Stack 4 was fabricated with matching layer Eccosorb MF112. Figure 4.13 shows the electrical impedance measurement in air for Stack 4 in blue, with a wire connected in green and with wire and housing and wire connected in red. Result from Mason model is shown by the black dashed line. Fitted parameters for PZ29 and material parameters from table was used for the Mason model. The pink dashed line shows result from COMSOL simulation, where the complex loss terms were used.
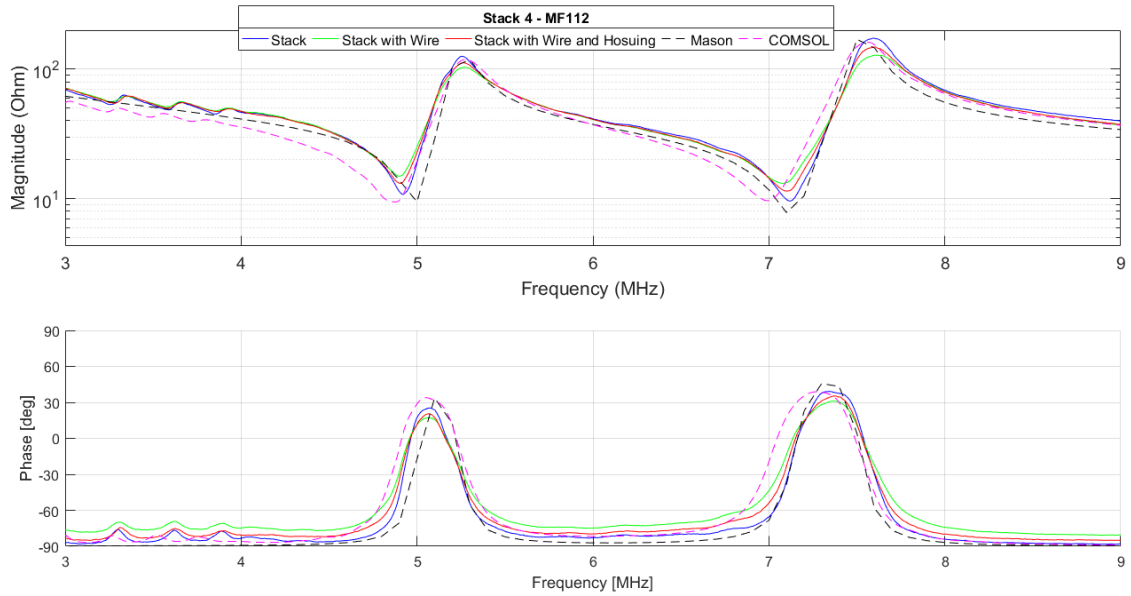
Figure 4.13 – Electrical impedance measurement on Stack 4 alone in blue, with wire in green and with wire and housing in red. Mason model result in black dashed line, COMSOL simulation result in pink dashed line. Fitted parameters for PZ29 was used for the Mason model. Complex loss terms were used for the COMSOL model.

4.2.6   Electrical Impedance of Stack 5, 6 and 7

Figure 4.14 shows the electrical impedance measurement of three unsuccessful transducer stacks. The piezoelectric element was not bonded correctly to the matching layer, causing significant thickness deviations over the surface. The measured impedances are compared to the ideal electrical impedance calculated from the Mason Model shown by the black dashed line.
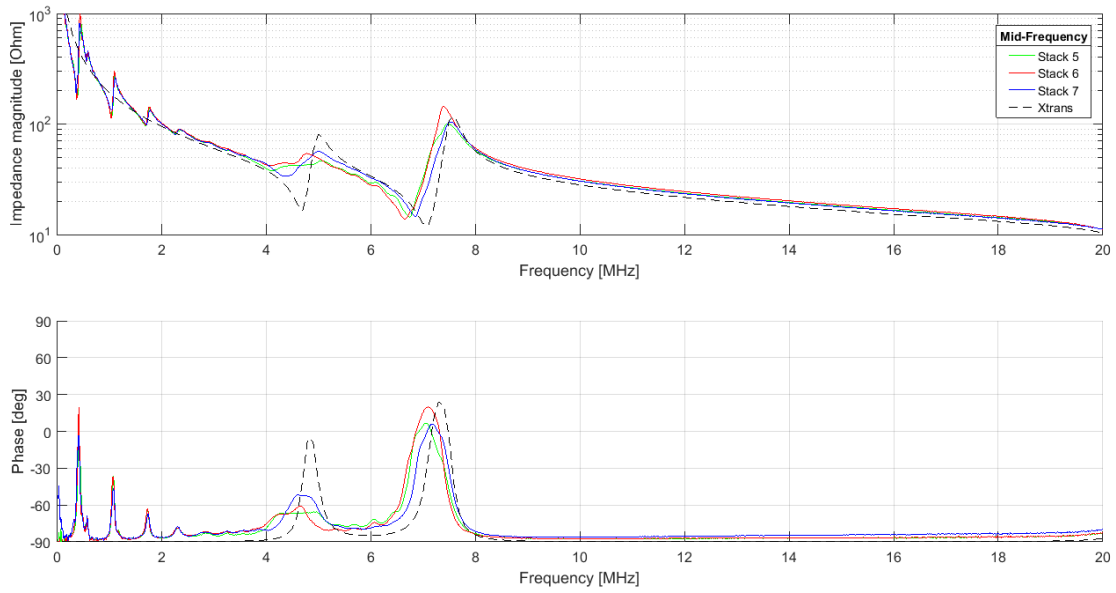
Figure 4.14 – Electrical impedance measurement on Stack 5, 6 and 7. The stacks were unsuccessful due to improper bonding between piezoelectric element and matching layer.

4.2.7 Pulse-Echo Measurement

The transmit transfer function for transducer Stack 3, Stack 4 and Lapped Stack 2 was measured using the pulse echo setup. Figure 4.15, 4.16 and 4.17 shows the transmit transfer function to the left and the transmit transfer function normalized to maximum amplitude to the right. The measured results are shown in red, Mason model is shown in blue.

Figure 4.15 – Transmit transfer function for Stack 4 shown in red. Mason model calculation is shown in blue. Figure to the right shows the transmit transfer function normalized to max amplitude. -3dB bandwidth is 44%.

Figure 4.16 - Transmit transfer function for Stack 3 shown in red. Mason model calculation is shown in blue. Figure to the right shows the transmit transfer function normalized to max amplitude. -3dB bandwidth is 20%.
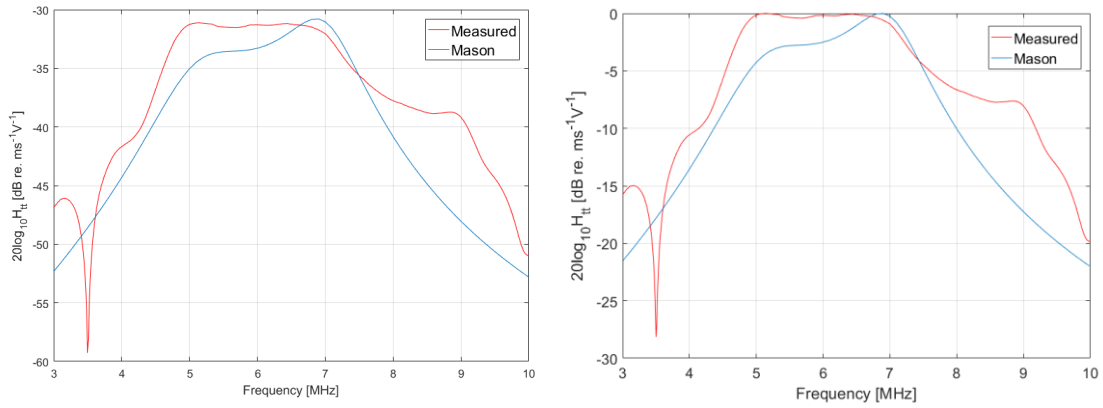

Figure 4.17 - Transmit transfer function for Lapped Stack 2 shown in red. Mason model calculation is shown in blue. Figure to the right shows the transmit transfer function normalized to max amplitude. -3dB bandwidth is 49%.
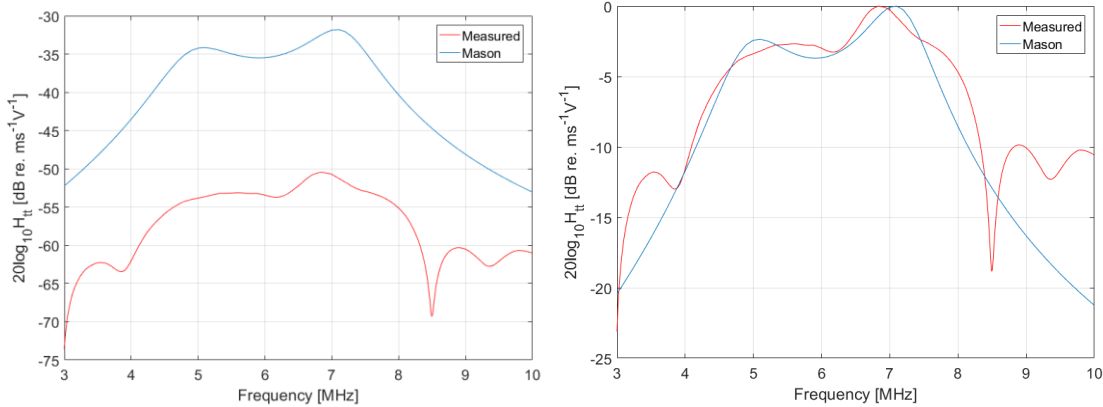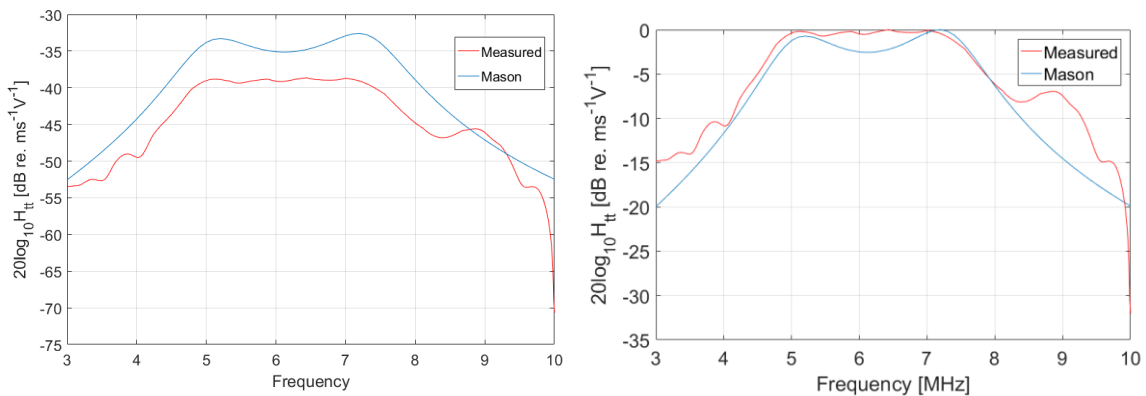
4.3 High-Frequency Single Element Transducers

4.3.1 Fabricated High-Frequency Needle Transducer

The approach of fabricating transducers housed in a stainless steel tube was successful. The transducers were completed and was characterized by electrical impedance measurements and beam profile measurements. Table 4.8 shows the specifications of the fabricated transducers.

Table 4.8 – Build Specification for High Frequency Needle Transducers

|	PZT5-H	PMN-PT
Yield	5 transducers	1 transducer
Housing	Stainless steel needle with 45-degree opening angle. Inner diameter: 1.75 mm Outer diameter: 2 mm	
Connection	Coaxial cable to ¼" SMA adapter	
Piezoelectric element thickness	90 µm	100 µm
Electrode thickness	Chrome: 200 nm Gold: 500 nm	
2-3µm silver epoxy thickness (1st matching layer)	27 µm	28 µm
Parylene thickness (2nd matching layer)	25 µm	25 µm
E-solder 3022 thickness (backing layer)	3.02 mm	1.67 mm
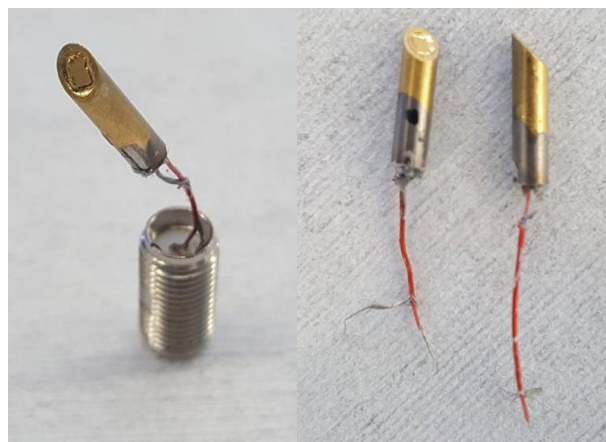
Figure 4.18 – Fabricated Needle Transducer

4.3.2 Comparison of Mason's Model and KLM Model

A high frequency transducer was simulated in two software packages: Xtrans (implementation of the Mason model) and PiezoCAD (implementation of the KLM model) in order to compare the similarities between the two models. The dimensions used for the two models were identical, using the thickness parameters listed in Table 4.9 and material parameters from Table 4.1 –Active Materials used for Mason Modeland Table 4.2 – Passive Materials Used For Mason Model. Result is shown in Figure 4.19.

Table 4.9 – Parameters for comparing Mason and KLM Model

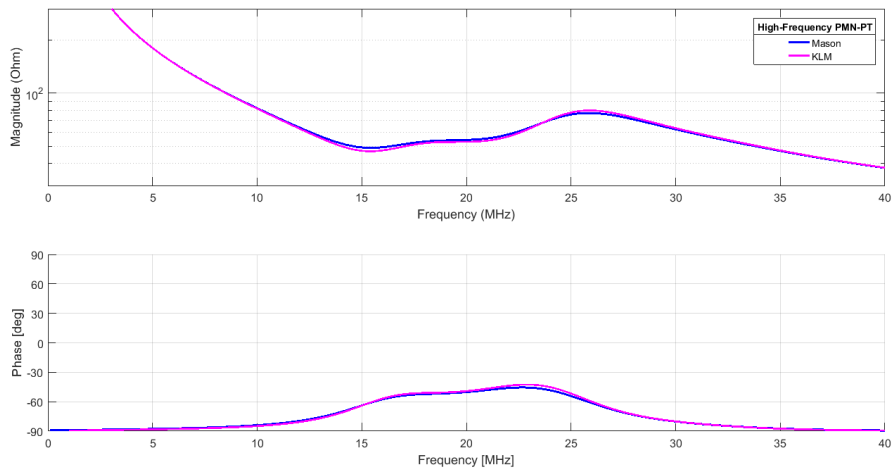| Model Parameters		
Backing	E-Solder	Infinite
Active Element	PMN-PT Thickness	95.55 µm
1st matching layer	2-3 Silver Epoxy	20 µm
2nd matching layer	Parylene	22µm
Load	Water	Infinite
Aperture	Disk	1.4 mm diameter

Figure 4.19 – Comparison of Mason model (blue) and KLM model (red).

The results are satisfactory, as the KLM and Mason model yield close to identical results. For further simulations, the Mason model is used to calculate electrical impedance.

4.3.3 Electrical Impedance of PZT5-H Needles

Figure 4.20 shows the electrical impedances of five PZT-5H transducers compared with the simulated electrical impedance of the mason model.
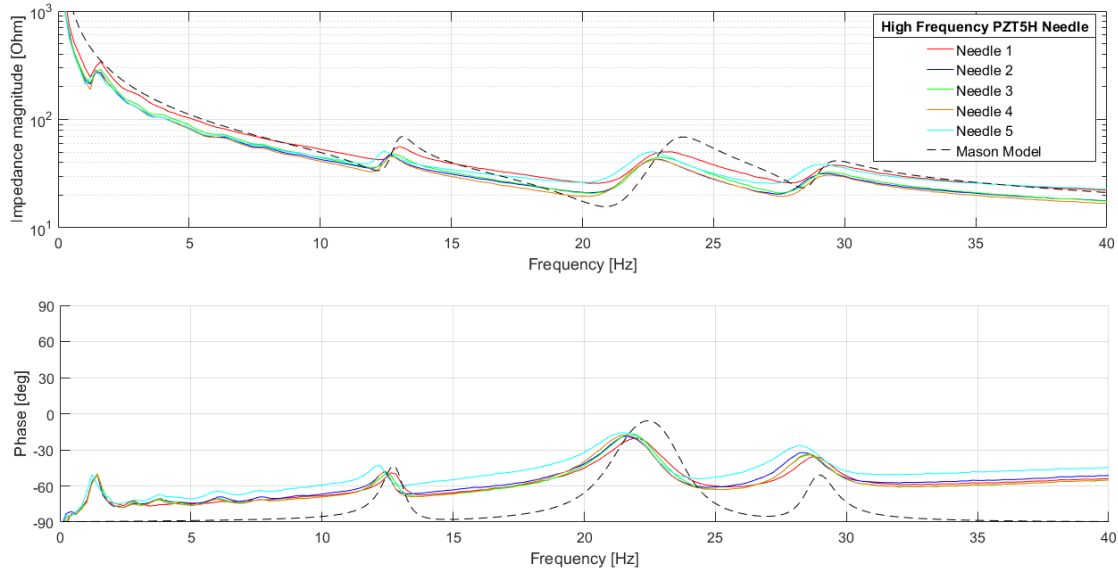
Figure 4.20 – Electrical impedance measurements in air on five PZT-5H Needle Transducers compared to Mason model in black dashed line.

The performance of the fabricated transducers match well with slight deviations, due to imperfect lapping of the different layers that make up the transducer. Some bias offset can be expected as the length of the coaxial wire varies for each element. The electrical impedance phase of Figure 4.20 indicates an offset in the phase from the measured transducers to the Mason model. The network analyzer was calibrated for only the SMA adapter so the wire and housing will have an influence on the measured electrical impedance.

An attempt at compensating for the electrical wire and housing was done by measuring their electrical impedance and subtracting these measured values in MATLAB. The result can be seen in Figure 4.21. As the impedance plot indicates, the offset was slightly reduced by calibrating for the housing and wire. Still a large offset is observed, which might be caused by the electrical impedance of the conductive matching layer and backing layer.
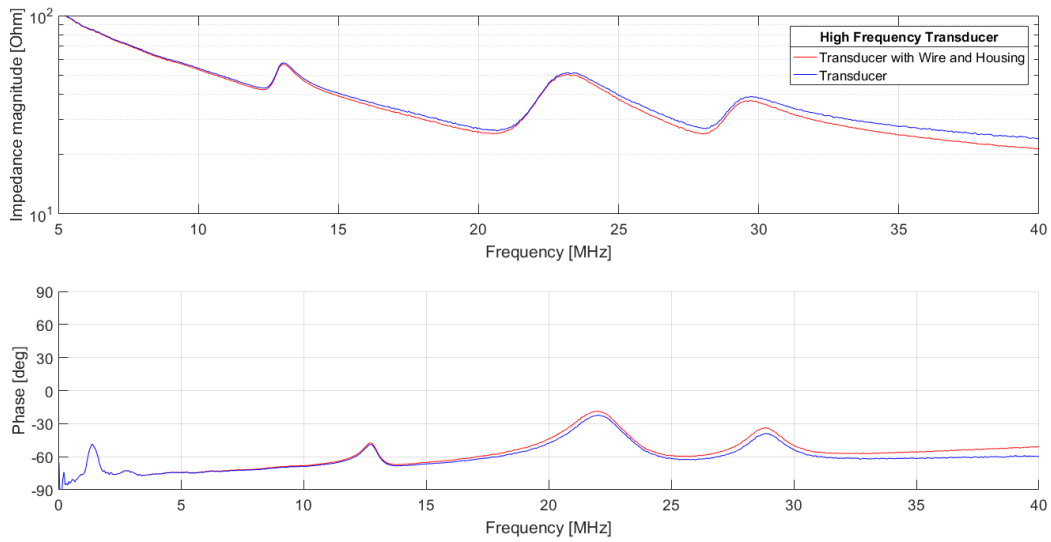
Figure 4.21 – PZT-5H Needle transducer compensated for wire and housing. Before compensation shown in red, after compensation shown in blue.

COMSOL was used to simulate the electrical impedance of the transducer. Figure 4.22 shows the result from two COMSOL simulations using material parameters listed in Table 4.3. The COMSOL simulation results are compared to the Mason model and the measured electrical impedance of one of the transducers.
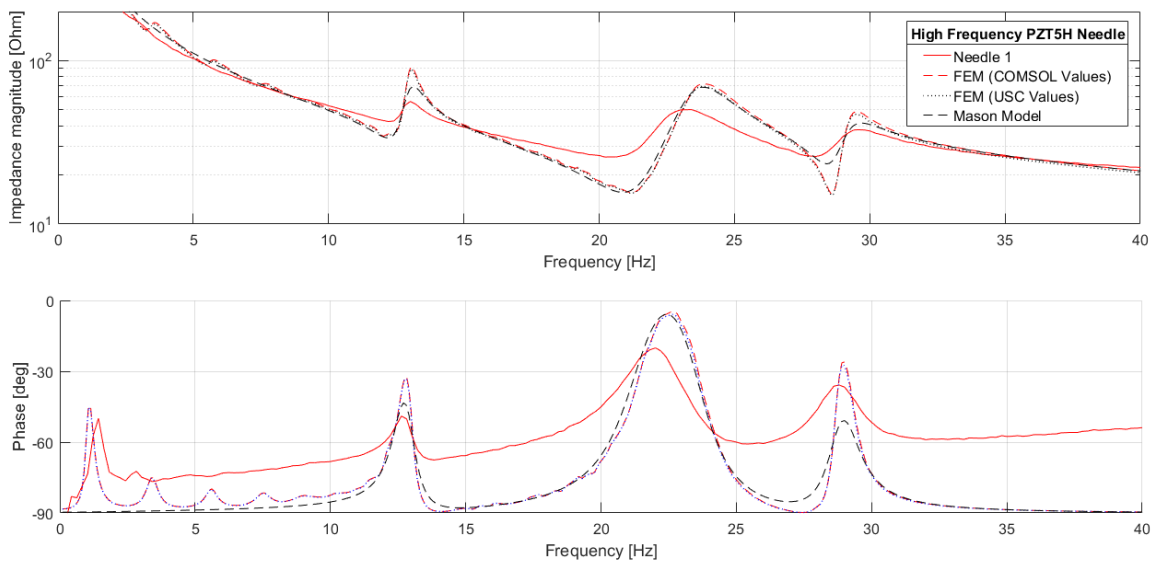
Figure 4.22 – COMSOL simulation results of PZT-5H Needle transducer in red dashed line and black dotted line are identical. Mason model in black dashed line and measured transducer in red line.

The two datasets used for the COMSOL simulation were similar and the result of the simulations is identical. A deviation between COMSOL and the Mason model was

observed at the third harmonic. The measured electrical impedance indicate the fabricated transducers were heavily damped.

4.3.4 Electrical Impedance of PMN-PT Needles

Electrical impedance measurement on the PMN-PT needle transducers indicated an error as the transducers did not resonate at all. It was theorized that this could be a caused by the piezoelectric PMN-PT material being unpoled. Either the material had not been poled prior to fabrication, or the poling was destroyed during heat treatment of the element.

A high voltage DC voltage was applied across two PMN-PT transducers as an attempt at repoling the piezoelectric element. One of the transducers showed no response to the repoling, while the last element was successfully repoled. Figure 4.23 shows the electrical impedance of the PMN-PT transducer before and after repoling, plotted in red and blue, respectively.
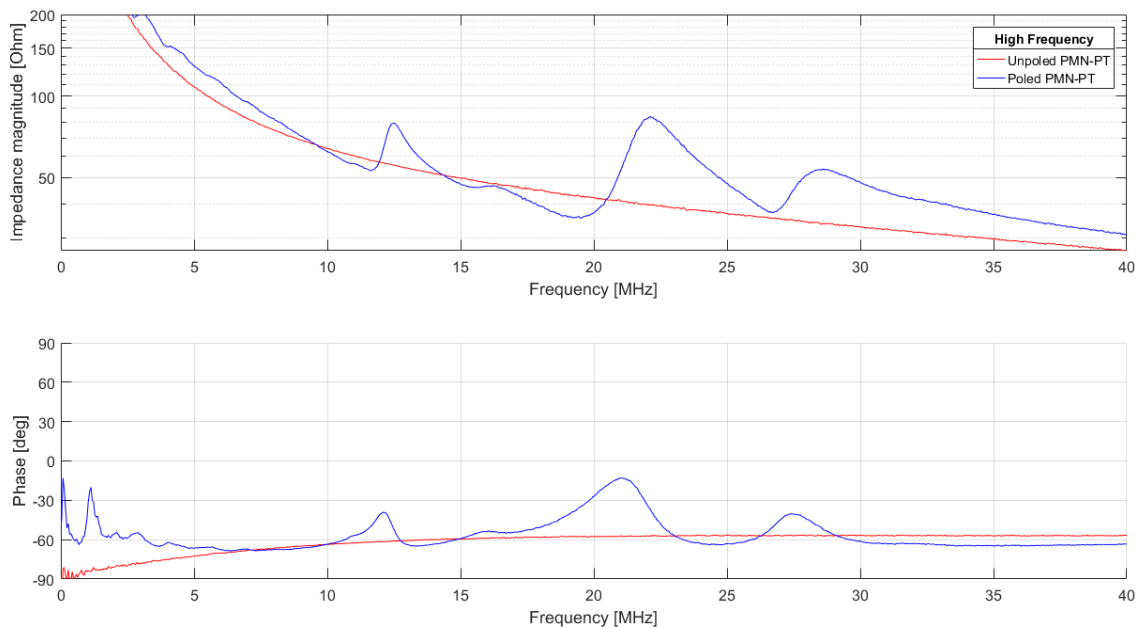
Figure 4.23 – Before and after poling PMN-PT Needle Transducer shown in red and blue, respectively. The transducer was poled using a DC waveform with 80V amplitude.

As seen in Figure 4.23, the repoling of the element was successful. The slight bias offset between the unpoled and poled transducer, as seen in the impedance magnitude plot at 5 MHz was due to the wire of the transducer being cut and stripped between the two measurements. This had to be done in order to connect the transducer to the voltage source for repoling.

The measured electrical impedance of the poled PMN-PT was compared to the Mason model and COMSOL simulation, as shown in Figure 4.24.
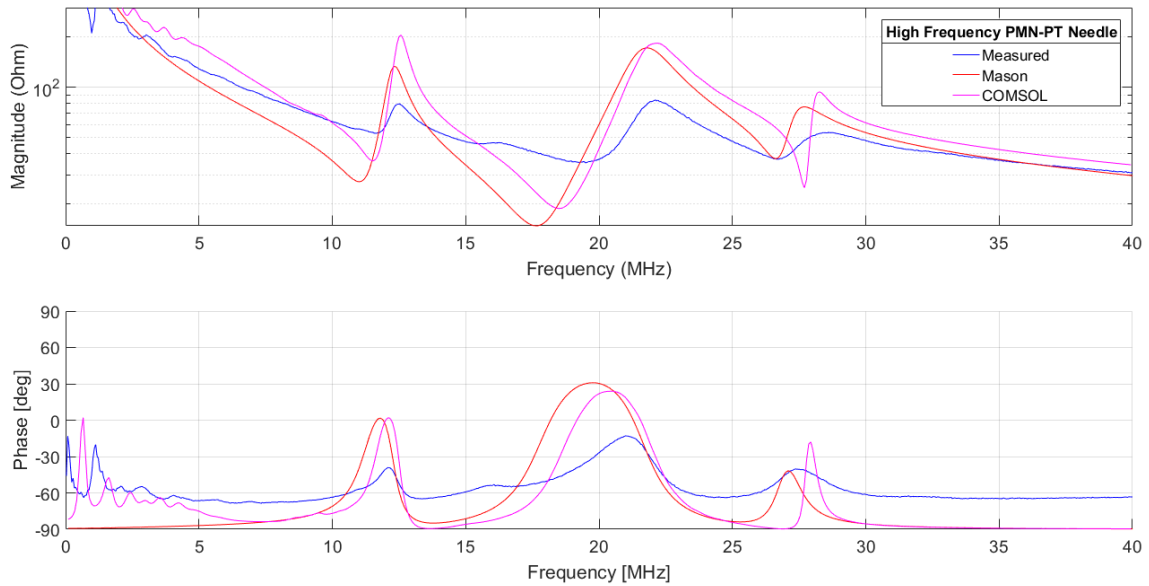
Figure 4.24 – Electrical impedance of PMN-PT Needle Transducer. Blue line shows the measured result. Red line shows the result from the Mason model. Pink line shows the COMSOL simulation result.

4.3.5 Beam Profile Measurement

The beam profile of the high frequency needle transducers (PZT-5H and PMN-PT) was measured using the Onda system. The lateral plane (X, Y) was measured for varying distances (Z). Figures below show the pulse energy in dB relative to maximum along with the pulse received by the hydrophone at the center of the beam in time-domain. Measured beam pattern is compared to Field II simulations along with the impulse response for the transducer.
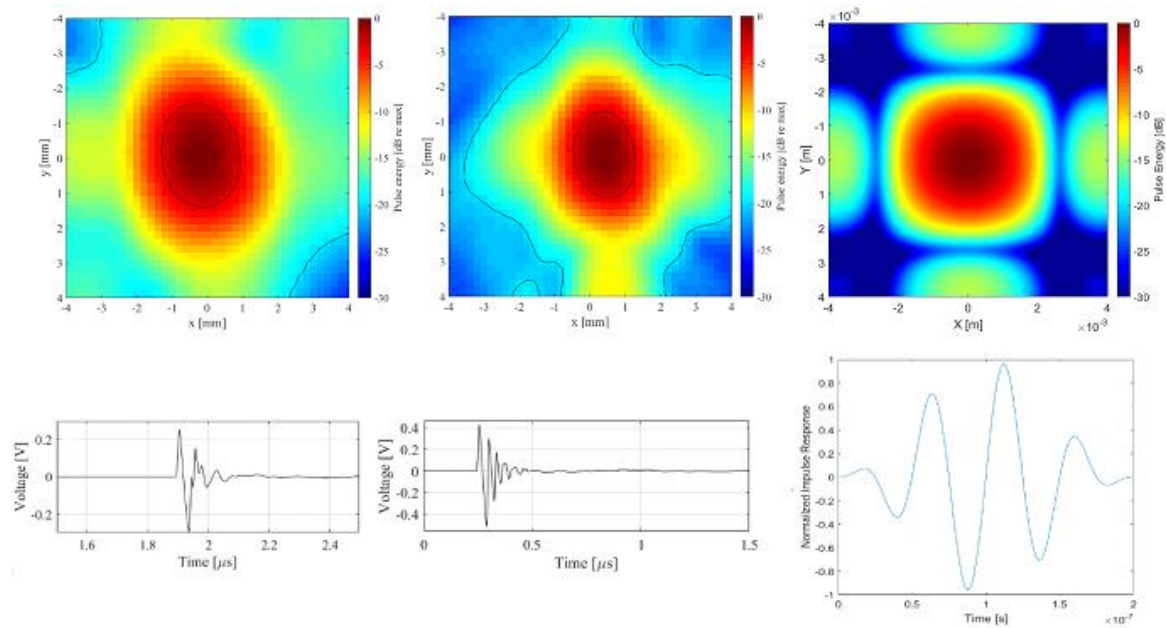
Figure 4.25 – Lateral plane measured at a distance Z=20mm from the transducer. From left, PZT-5H, PMN-PT, Field II. Figures on top show the pulse energy in dB relative to maximum. Figures on bottom show the pulse received by the hydrophone at the center of the beam in time-domain.
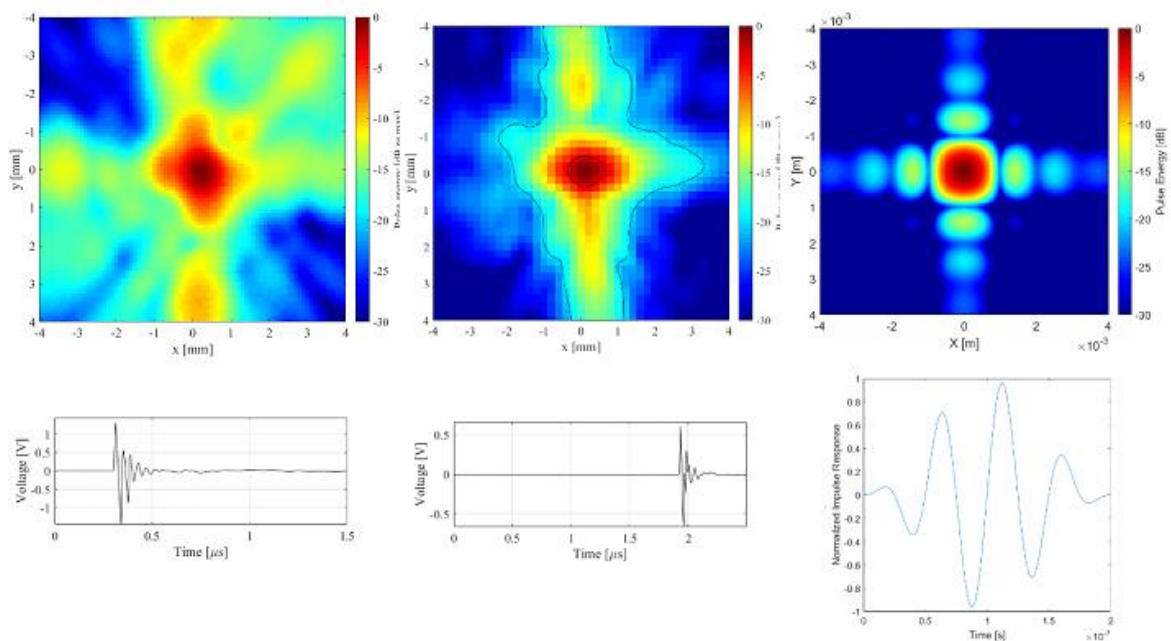
Figure 4.26 – Lateral plane measured at a distance Z=7.5 mm from the aperture. From left, PZT-5H, PMN-PT, Field II. Figures on top show the pulse energy in dB relative to maximum. Figures on bottom show the pulse received by the hydrophone at the center of the beam in time-domain.
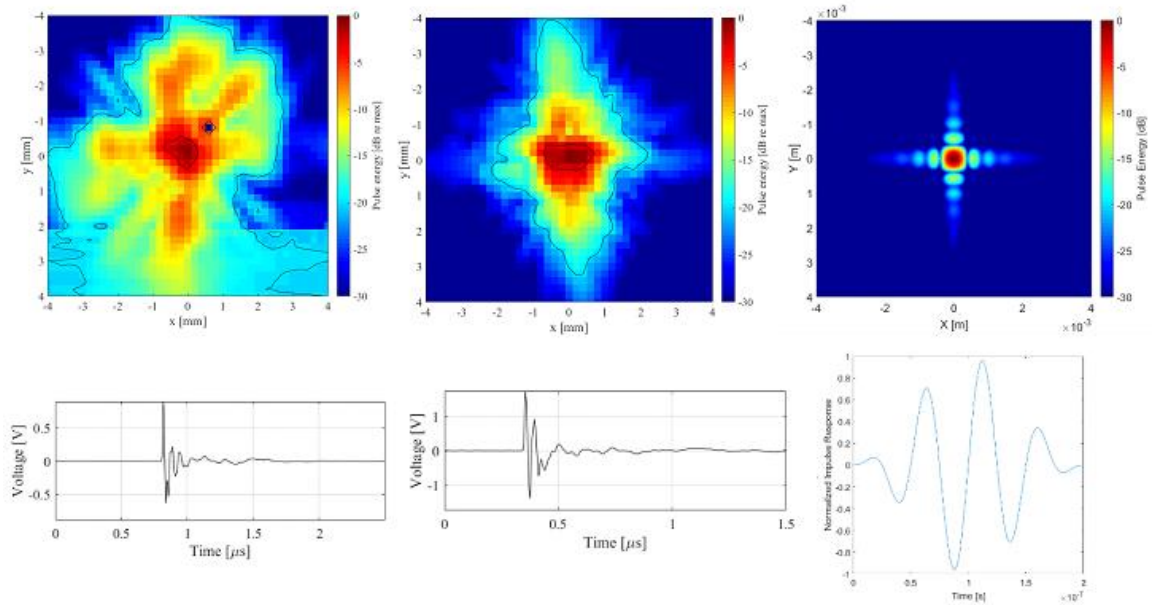
Figure 4.27 –Lateral plane measured at a distance Z=3 mm from the aperture. From left, PZT-5H, PMN-PT, Field II. Figures on top show the pulse energy in dB relative to maximum. Figures on bottom show the pulse received by the hydrophone at the center of the beam in time-domain.

4.4 High-Frequency Single Element Copper Sheet Transducer

The approach of fabricating an air-backed high frequency transducer was unsuccessful. The transducer released from the copper sheet during the last dicing step due to poor adhesion between the copper and E-solder. As a result, there was no longer contact with the bottom electrode of the piezoelectric element. The transducers were not completed and could not be characterized.

4.4.1 Fabricated High-Frequency Copper Sheet Transducer

	PZT5-H	PMN-PT
Yield	Multiple, non-functioning	Multiple, non-functioning
Connection	Coaxial cable	Coaxial cable
Piezoelectric element thickness	90 µm	100 µm
Electrode thickness	Chrome: 200 nm Gold: 500 nm	
2-3µm silver epoxy thickness (1st matching layer)	27 µm	28 µm
Parylene thickness (2nd matching layer)	25 µm	25 µm
E-solder 3022 thickness (bonding layer)	31 µm	27 µm
Copper sheet thickness	33 µm	33 µm

Figure 4.28 – Fabricated "Copper Sheet" transducer. Top view of transducer to the left, bottom view of the transducer to the right.

5 Discussion

5.1 Mid-Frequency Single Element Transducers

5.1.1 Fabricated Mid-Frequency Transducers

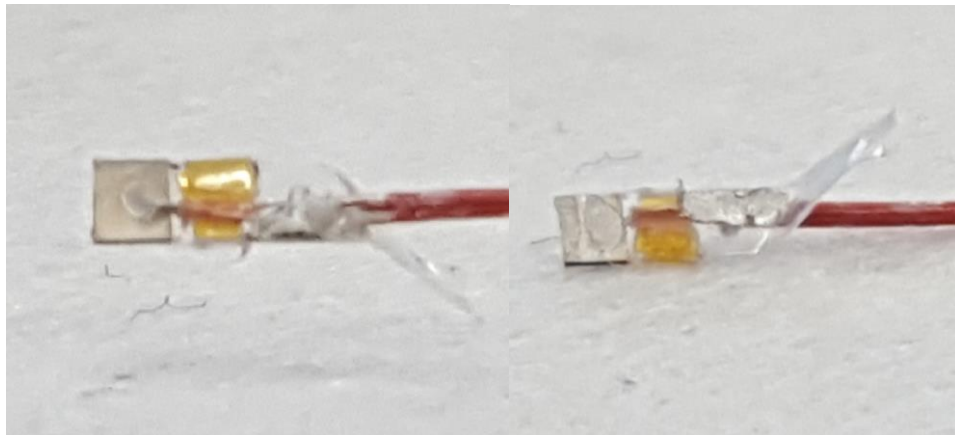The variation in matching layer thickness will have an influence on the performance of the transducer. It was difficult to obtain the desired matching layer thickness with the lapping equipment. A safe thickness was achieved and used in order to avoid overlapping. The matching layer for one transducer was later lapped down to the desired thickness of 85 µm.

The bonding layer will influence the performance of the transducer. According to Xtrans calculations, a thick bonding layer would decrease sensitivity, so a thin bond line was desired. The use of a thin non-conductive bonding layer has been proven to work.

The pint head of the 3D printer was 0.5 mm, which is quite poor for printing miniature structures. With a better resolution, smaller housings could have been fabricated to give a smaller footprint of the transducers. The sputtering of the matching layers and housings was unsuccessful in the first attempt. The plasma cleaning procedure caused the plastic housings to melt and deform. For a second batch, the plasma cleaning exposure time was reduced and the plastic did not melt.

Even though the packaging of the transducer is thought to be fragile, it proved otherwise. None of the packaged transducers broke or showed any signs of failure upon impedance measurements post-acoustic measurements.

5.1.2 Fitting Material Parameters

The piezoelectric ceramic showed slight thickness variation in some of the diced samples. It was shown that the thickness of the piezoelectric material has an influence on the resonance frequency, as expected from Equation (2.2).

The result from electrical impedance measurement on PZ29 deviated from the impedance calculated by the Mason model. As it can prove beneficial to have accurate datasets for estimating the performance of a transducer prior to fabrication, a fitting was in

order. Material parameters were fitted to match the measured impedance by manually changing the input data. A good match was found by reducing the mechanical loss factor Q_m and H_{33} from 195 to 80 and 19.2 to 16.5, respectively.

Next, a fabricated transducer was measured and compared to the Mason model. The comparison indicated a slight deviation in magnitude. A close match was obtained by decreasing the Q-factor for the matching layer from 38 to 20. The material parameters for the bonding layer were kept as they were, based on the assumption that the matching layer will dominate the influence since this layer is relatively thicker than the bonding layer.

Local dead zones can arise when the piezoelectric element is diced due to high temperatures, which could explain the deviation from what the manufacturer specified. However, deviation in material parameters from manufacturer's specifications is common.

5.1.3 FEM Simulations

Material parameters from Ferroperm A/S was used to describe the piezoelectric material PZ29. Two approaches to account for the losses were compared. One using complex loss fitted for PZ27, and another simplified model by defining an isotropic loss using the mechanical loss factor for PZ29. The approach of using the complex loss components for PZ27 in the FEM simulations was found to be superior to the simplified FEM model described with isotropic loss. The model described with isotropic loss did not account for the dielectric loss and showed frequent dips in Figure 4.7. The model described with complex loss did account for the dielectric loss and resulted in a smoother curve.

The one-dimensional model and simplified FEM model indicated a higher impedance magnitude, meaning the loss in the simulations was too low. A shift in frequency was observed when comparing the simulation to measurement. Simulations indicated a resonance peak at 6 MHz while the actual resonance peak was at 6.25 MHz.

The COMSOL simulation of Stack 1,2,3 shown in Figure 4.8 indicated a higher impedance magnitude and phase than what was measured for the fabricated transducers. Simulation result for Stack 4, in Figure 4.13, did however result in a close match between simulation and measurement result. The matching layer material used was the only

difference between in the two simulations, giving reason to believe this might be the source of error.

5.1.4 Electrical Impedance Measurement

The 1D model is valid because the transducer's diameter is much larger than its thickness. Electrical impedance of the fabricated transducers were measured and studied for influence of electrical connections. As the electrical impedance magnitude is higher than 50Ω, electrical matching could be employed to further increase sensitivity of the transducers. Electrical impedance measurements were frequently performed throughout the fabrication procedure for evaluating the influence of adding layers, electrical connections and packaging. No significant effect were observed when housing the transducers, indicating that the piezoelectric elements were not clamped by the wall of the housing.

5.1.5 Pulse Echo Measurements

The transducer's transmit transfer function was measured using the pulse echo setup. The results indicated that Stack 4 and Lapped Stack 2 had the best performance with a -3dB bandwidth of 42% and 49% , as well as a close match to the calculations from the Mason model. Stack 2 was initially identical to Stack 3 before lapping. The transmit transfer function of transducer Stack 3 was however very low, with a -3dB of 20% and a large mismatch between measurement and Mason model. Regarding the mismatch between measured transducer Stack 3 and Mason model, this could be caused by the thickness of the matching layer being higher than a quarter wavelength, hence not optimal transmission. Another explanation is that it could be caused by measurement error.

5.2 High-Frequency Single Element Transducers

5.2.1 Fabricated Needle Transducers

The fabrication of high frequency transducers in the USC biomedical engineering lab were different from that of HSN. The time required to finalize a transducer was much longer.

Prior to fabrication, the thickness dimensions of the transducer were decided through simulations in PiezoCAD, using the KLM method. The aperture size was determined based on Field II simulations of the beam profile. The transducers were

designed with a center frequency of 20 MHz in water with a bandwidth of approximately 50%.

All lapping was done manually by hand which allowed for much more precision in the thicknesses obtained. Working with samples with thickness about 100 µm proved to be difficult. Several samples of PMN-PT broke during handling, which decreased the final yield.

The matching and backing layers were cast directly onto the piezoelectric element. This avoids the need for a bonding layer which would decrease the sensitivity of the transducer. Higher frequency requires a thinner piezoelectric element. This thin element has to have some form of mechanical support in order not to break, so backing layer was used. The backing layer will give an increase in bandwidth on the cost of sensitivity.

The housing of the transducer was made of a stainless steel tube which was cut with a 45 degree opening angle. This opening angle will allow the transducer to be placed perpendicular to a blood vessel and still being able to obtain blood flow information as the angle accounts for the Doppler angle, described in section 1.1.

Electrical impedance measurements could only be done once the transducer was completed in a housing and connected to the SMA adapter. As each new layer is cast on the transducer, no information can be obtained about the influence of the layer applied.

The lab was equipped to perform pulse-echo measurements for high frequency transducers. However, due to limited time this could not be realized.

5.2.2 Fabricated Copper Sheet Transducers

The purpose of this design was to reduce the total thickness of the transducer and to avoid the use of a backing material for increased sensitivity. A piezoelectric element with a matching layer cured over the front surface was bonded to a copper sheet. Connections to the electrode would be made by connecting wires to the copper sheet and the conductive matching layer. This was an original design that had not been attempted by the USC ultrasound group before. Fabrication of the copper sheet transducers were not successful.

The piezoelectric element and matching layer was prepared following the standard procedure. The piezoelectric element with a matching layer was then to be bonded to the copper. First a non-conductive epoxy was used with no success, the element released from

the copper directly after curing due to weak adhesion. Next, a conductive silver epoxy was used to bond the element.

The conductive epoxy would several times short circuit the transducer due to contact with the top surface of the transducer as the element was pressed down to reduce the bond thickness. At last, the element was successfully bonded using conductive epoxy without pressing. Wires were connected to the conductive matching layer and copper sheet. In the last step, the larger sample were to be diced out in the final aperture size. Due to vibrations from the dicing blade, the poor adhesion caused the element to release from the copper sheet. There were no longer contact with the bottom electrode of the transducer.

A decision was made to discard this design in favor of the needle design. These elements were not characterized.

The transducer should be bonded with a thin bondline to a copper sheet with rough surface. 4MHz transducers have been successfully fabricated at the HSN ultrasound lab by bonding the piezoelectric element to a 18 µm copper sheet using non-conductive 3M DP460 epoxy.

5.2.3   Poling PMN-PT Needle Transducer

Electrical impedance measurements of the PMN-PT needle revealed the PMN-PT material was not poled. There are two possible explanations for this; the PMN-PT had not been polarized before the sample was assigned or the element had become unpoled due to heating during fabrication. The latter is less likely since temperatures did not rise above 70 degrees, which is much lower than the Curie temperature.

The PMN-PT needle transducer was successfully poled. The electrical impedance curves of the element before and after poling was measured and compared. The unpoled transducer resembled a capacitor, with no resonance peaks. Clear resonance peaks were apparent after poling.

5.2.4   FEM Simulations of High-Frequency Transducers

Two similar datasets were used to model the PZT-5H in FEM. The first dataset was taken from the COMSOL Library for piezoelectric materials, and the second dataset was provided from the USC group. The two datasets were quite similar and gave identical

results. The loss for the piezoelectric material was defined as isotropic, using only the mechanical loss factor Q_m.

Material parameters found in literature was used to model the PMN-PT transducer. The COMSOL simulations results indicate a mismatch to measured results, as well as the Mason model. Small variations in thickness become more apparent for higher frequencies. However, the mismatch between simulations and measurements indicate that the actual loss is greater than what is defined in the COMSOL and Mason model. A closer inspection of the material parameters should be looked into for accurate predictions of the transducer performance.

5.2.5 Electrical Impedance Measurement

The electrical impedance of the high frequency needle transducers are heavily damped. This will decrease the sensitivity of the transducers. Inductance, likely caused by electrical connections is apparent. The needle housing and wire a PZT-5H transducer was compensated for, yet the inductance is clearly visible. This could be explained by the conductive backing material in the transducer.

5.2.6 Beam Profile Measurement

Beam Profile measurement were performed with the high frequency needle transducers. Aligning the transducer with the Z axis, as well as the X and Y axis proved to be challenging due to the small size of the transducer. The Onda system will correct for a small misalignment angle in the Z direction, however no alignment for the X and Y axis. The aperture had to be aligned with the X- and Y-axis in order to obtain symmetric results.

A dirac delta function was used to excite the transducer during measurement. Ideally, a sine function should be used, but the instruments in the lab were not suited for the high frequencies. The Onda hydrophone was calibrated in the range from 900 kHz to 20 MHz. Hence, the measurements are slightly out of range. Beam patterns are seen to resemble the cross-patterns, characteristic for square or rectangular apertures.

6 Conclusion

In this thesis, mid- and high frequency transducers were designed, fabricated and characterized. One-dimensional equivalent circuit model and 2D FEM simulations were compared to measurements on fabricated transducers.

Miniature 6 MHz mid-frequency transducers were fabricated in two versions by employing matching layers of different acoustic impedance. Square elements of PZ29 was used for the active element in the transducers. Transducers were optimized for high sensitivity with a narrow beam pattern. A new design for housing the transducers was suggested, by mounting the transducer unclamped in a housing. The transducers were characterized by electrical impedance measurements and pulse-echo measurements were performed on selected transducers to study the transmit transfer function. The best performing mid-frequency transducer had a -3dB bandwidth of 49% and a high sensitivity due to air backing.

Material parameters for PZ29, the active element used in the mid-frequency transducers, and Eccosorb MF114, used as one of the matching layer materials, was fitted in the Mason equivalent circuit model to match measured results.

Miniature high frequency transducers were fabricated at the Biomedical Research Center of University of Southern California. Two designs were approached where only one of them was successful. The transducers were designed to operate at 20 MHz center frequency with 50% bandwidth. PMN-33PT and PZT-5H was used as the active material for the high frequency transducers. The successful design employed two matching layers and a backing material. The transducer was housed in a stainless steel needle with 45-degree opening angle. Electrical impedance measurements were compared to one-dimensional Mason model and 2D FEM simulations. The lateral beam profile was measured and compared to Field II simulations. A second design for the high-frequency transducers was approached. The transducer was designed to be side-facing using air backing, giving the transducer high sensitivity and relatively low thickness. This design was unsuccessful and was not characterized.

6.1 Future Work

Based on the results presented in this thesis, several interesting directions for future work are described below.

- Fabricating a transducer with electrical matching to further increase sensitivity.
- Fabricating an air-backed high frequency transducer.
- Fabricating a low frequency PMN-PT transducer.
- Fitting PZ29 material data for FEM model.
- Characterizing PMN-33PT material.
- Performing pulsed-wave Doppler measurements.

References

[1] - A. R. Koosha and Y. S. Sunthankar, "Digital transmission in water," in *IEEE 1991 Ultrasonics Symposium,* 1991, pp. 1035–1038 vol.2.

[2] W. Jiang and W. M. D. Wright, "Wireless communication using ultrasound in air with parallel OOK channels," in *24th IET Irish Signals and Systems Conference (ISSC 2013)*, 2013, pp. 1–6.

[3] - J. Krautkrämer and H. Krautkrämer, *Ultrasonic testing of materials*. Springer-Verlag, 1983.

[4] - K. K. Shung, *Diagnostic Ultrasound: Imaging and Blood Flow Measurements*. CRC Press, 39-55, 2005.

[5] W. G. Pitt, G. A. Husseini, and B. J. Staples, "Ultrasonic Drug Delivery – A General Review," *Expert Opin Drug Deliv*, vol. 1, no. 1, pp. 37–56, Nov. 2004.

[6] V. A. Khokhlova, L. A. Crum, G. ter Haar, and J. F. Aubry, *High Intensity Focused Ultrasound Therapy - Fundamentals through Clinical Challenges*. Springer International Publishing.

[7] A. Carovac, F. Smajlovic, and D. Junuzovic, "Application of Ultrasound in Medicine," *Acta Inform Med*, vol. 19, no. 3, pp. 168–171, Sep. 2011.

[8] Satomura S, Matsubara S, Yoshioka M. A new method of mechanical vibration measurement and its application. Mem Inst Sci Ind Res Osaka Univ. 1956;13:125

[9] I. M. Coman and B. A. Popescu, "Shigeo Satomura: 60 years of Doppler ultrasound in medicine," *Cardiovasc Ultrasound*, vol. 13, Dec. 2015.

[10] D. Popovici, F. Constantinescu, M. Maricaru, F. I. Hantila, M. Nitescu, and A. Gheorghe, "Modeling and Simulation of Piezoelectric Devices," 2008.

[11] P. Dineva, D. Gross, R. Müller, and T. Rangelov, *Dynamic Fracture of Piezoelectric Materials*, vol. 212. Cham: Springer International Publishing, 2014.

[12] Lawrence E. Kinsler, Austin R. Frey, Alan B. Coppens, and James V. Sanders, Fundamentals of Acoustics. New York: John Wiley & Sons, 1982

[13] Desilets CS, Fraser JD, and Kino GS, "The design of efficient broad-band piezoelectric transducers," IEEE Trans Sonics and Ultrasonics SU-25, 115–25, 1978.

[14] W. P. Mason, *Electromechanical transducers and wave filters*. D. Van Nostrand Co., 1948.

[15] R. Krimholtz, D. A. Leedom, and G. L. Matthaei, "New equivalent circuits for elementary piezoelectric transducers," Electron. Lett., vol. 6, no. 13, pp. 398–399, Jun. 1970.

[16] S. Sherrit, S. P. Leary, B. P. Dolgin, and Y. Bar-Cohen, "Comparison of the Mason and KLM equivalent circuits for piezoelectric resonators in the thickness mode," in *1999 IEEE Ultrasonics Symposium. Proceedings. International Symposium (Cat. No.99CH37027)*, 1999, vol. 2, pp. 921–926 vol.2.

[17] T. Franke Johansen and T. Rommetveit, "Characterization of Ultrasound Transducers". Available: https://www.researchgate.net/publication/268243011_Characterization_of_Ultrasound_Transducers. [Accessed: 30-Jun-2017].

[18] J. A. Jensen and N. B. Svendsen. Calculation of pressure fields from arbitrarily shaped, apodized, and excited ultrasound transducers. IEEE Trans. Ultrason., Ferroelec., Freq. Contr., 39:262–267, 1992.

[19] J. A. Jensen. Field: A program for simulating ultrasound systems. Med. Biol. Eng. Comp., 10th Nordic-Baltic Conference on Biomedical Imaging, Vol. 4, Supplement 1, Part 1:351–353, 1996b.

[20] Q. Zhou, K. H. Lam, H. Zheng, W. Qiu, and K. K. Shung, "Piezoelectric single crystals for ultrasonic transducers in biomedical applications," *Prog Mater Sci*, vol. 66, pp. 87–111, Oct. 2014.

[21] "FEM modeling: Comsol Multiphysics and Elmer." [Online]. Available: http://nanophysics.pl/comsol.php. [Accessed: 01-Jul-2017].

[22] R. Zhang, B. Jiang, and W. Cao, "Elastic, piezoelectric, and dielectric properties of multidomain 0.67Pb(Mg1/3Nb2/3)O3 – 0.33PbTiO3 single crystals," in *Journal of Applied Physics*, Volume 90, Number 7, 2001, pp. 3471–3475.

[23] - M.Aanes, E. Storheim, M. Vestrheim, and P. Lunde, "Finite element analysis and measurements of ultrasonic piezoceramic transducers in air and water."

[24] S. Sherrit and H. D. Wiederick, "Non-Iterative Evaluation of the Real and Imaginary Material Constants of Piezoelectric Resonators," in *Ferroelectrics*, vol. 134, Gordon and Breach Science Publishers S.A., 1992, pp. 111–119.

[25] Hoa T. K. Tran, "Characterization of Acoustic Material Properties Using Broadband Through-Transmission Technique". Master Thesis, Høgskolen i Sørøst Norge 2016.

[26] K. C. Cheng, H. L. W. Chan, C. L. Choy, Q. R. Yin, H. S. Luo, and Z. W. Yin, "Piezoelectric Coefficients of PMN-0.33PT Single Crystal," in *0-7803-5940-2/01/$10*, IEEE, 2001, pp. 533–536.

[27] Q. Zhou *et al.*, "PMN-PT single crystal, high-frequency ultrasonic needle transducers for pulsed-wave Doppler application," *IEEE Transactions on Ultrasonics, Ferroelectrics, and Frequency Control*, vol. 54, no. 3, pp. 668–675, Mar. 2007.

[28] J. M. Cannata, T. A. Ritter, W.-H. Chen, R. H. Silverman, and K. K. Shung, "Design of efficient, broadband single-element (20-80 MHz) ultrasonic transducers for medical imaging applications," *IEEE Trans Ultrason Ferroelectr Freq Control*, vol. 50, no. 11, pp. 1548–1557, Nov. 2003.

[29] Duy Le Anh, "Investigation of Element Variance in Ultrasound Arrays by Electrical Impedance Measurements". Master thesis, Høgskolen i Sørøst Norge, 2016.

[30] "UT Material Properties Tables." [Online]. Available: https://www.nde-ed.org/GeneralResources/MaterialProperties/UT/ut_matlprop_metals.htm. [Accessed: 30-Jun-2017].
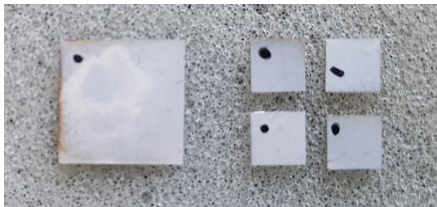
[31] "Acoustic impedance - Wikipedia." [Online]. Available: https://en.wikipedia.org/wiki/Acoustic_impedance. [Accessed: 30-Jun-2017].
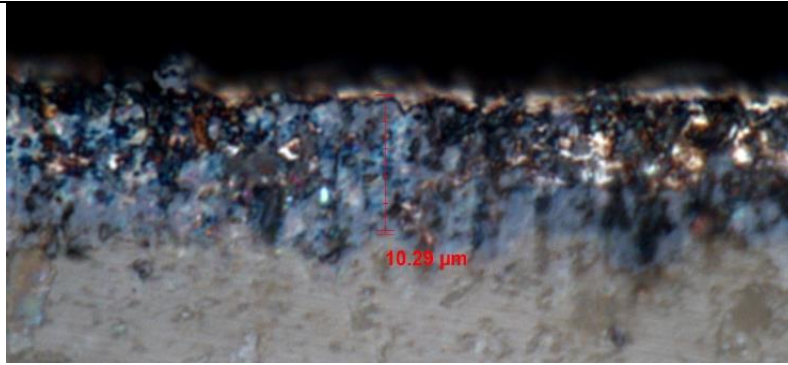
[32] "UT Material Properties Tables." [Online]. Available: https://www.nde-ed.org/GeneralResources/MaterialProperties/UT/ut_matlprop_liquids.htm. [Accessed: 30-Jun-2017].

[33] M. Messer, "Pulsed ultrasonic doppler velocimetry for measurement of velocity profiles in small channels and capplilaries," Thesis, Georgia Institute of Technology, 2005.

Appendix

A: Fabrication of Mid-Frequency Transducers

Step	Explanation	Data
1	Square plates of PZ29 with dimensions 3*3mm were diced by Alied Technologies dicing machine into squares of 4.2*4.2mm. The electrical impedance of the diced elements was measured with network analyzer HP 8753D (Agilent Technologies Inc. Philadelphia, PA). The thickness of all diced samples were measured.	Material: PZ29 Width, Length: 4.2mm, 4.2mm Thickness: 318 µm +- 2µm
2	Optical microscopy was used to evaluate the thickness of the electrodes on the piezoelectric element. 3 measurements were taken on 3 different elements with 1000X magnification.	Total thickness of piezoelectric: 318µm Electrode Thickness: 10µm +- 2µm

PZ29 before and after dicing. The marking on the element indicate the direction of polarization.

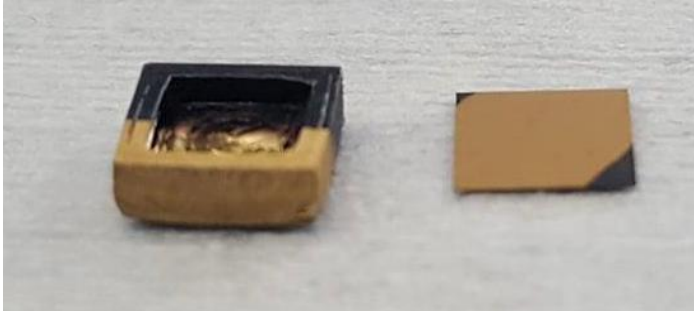Microscopy image of the silver painted electrode on PZ29.
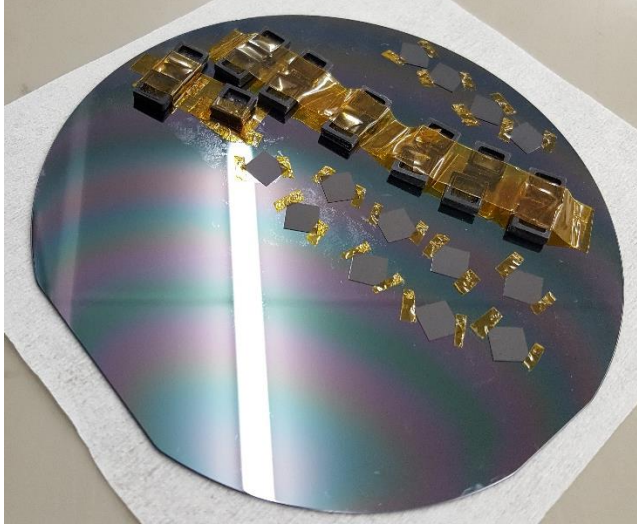
3	Eccosorb MF114 and Eccosorb MF112, the material used the matching layers, was cut out from a larger sample using a handsaw. The matching layers were wax bonded at 75 degrees Celsius to the chuck of the lapping machine. The matching layers were lapped. The thickness of the matching layers was checked evenly throughout the process by the thickness gauge.	Eccosorb MF114 thickness: 92µm +- 10µm Eccosorb MF112 thickness: 95µm +- 5µm
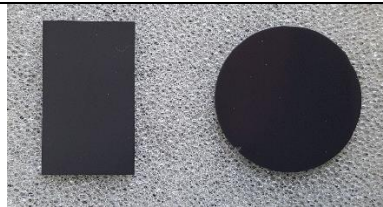
From left, Eccosorb MF114 and Eccosorb MF112 after lapping

4	The matching layers were diced to squares of 5.6*5.6mm.. The measure function on the machine was used to proof check the dimensions of the diced samples.	Matching layer width, height: 5.6mm, 5.6mm
5	Matching layers and piezoelectric elements were cleaned in the ultrasonic bath. The ultrasound bath was heated to approximately 60 degrees Celsius before placing the beakers with the liquids in the bath. Kapton cleaning of the matching	

72

	layers was necessary to remove all residue wax.
	Wax cleaner: 10 minutes (Kapton cleaning)
	2% Micron soap, 98% water mixture: 5 minutes
	DI water: 3 minutes (this cleaning was done twice in different beakers)
	Isopropanol: 5 minutes
	After each cleaning steps, except for the last, all samples were rinsed under running DI water for approximately 2 minutes. Compressed air was used to dry the elements after the last step.
	After cleaning, the samples were dried in at 60 degrees Celsius for 3 hours.
6	Solidworks, a 3D design software, was used to design a housing for the transducers along with a probe to use for acoustic measurements. Svein Midrebøe printed 15 samples of the housing and 3 samples of the probe with the 3D printer at HSN. The printed samples had to be polished by hand to give a smooth finish.

3D printed housings. Unpolished and polished housings at top and bottom, respectively.

|	3D printed probe. Unpolished and polished probe at top and bottom, respectively.	
7	The matching layers and the plastic housings were taped to a silicon wafer. Lab engineer, Anh Tuan Thai, preformed O_2 plasma cleaning for one minute before sputtering 25nm chromium and 150nm gold.	<u>O2 plasma cleaning:</u> 1 minute <u>Sputtering:</u> Chromium: 25nm Gold: 150nm
	Matching layers and housings prepared for sputtering process. 	
8	The thickness of a matching layer was measured before bonding it with 3M DP460 glue to one of the piezoelectric elements with the sputtered surface facing the unmarked surface piezoelectric element. The bonded sample was cured at 60 degrees Celsius under 20 Bar pressure for 3 hours. After curing, the electrical impedance was measured on the transducer stack.	<u>Bond layer thickness:</u> 2.5µm

9	A copper wire was connected to the underside of the piezoelectric element using conductive silver epoxy. The two components of the silver epoxy were mixed in the ratio 1:1. The silver epoxy was cured for 4 hour at 60 degrees Celsius in the thermal chamber.
	Three electrical impedance measurements were performed at this stage. First, the wire was measured by itself. Second, the wire and the housing together. After curing the silver epoxy connection, the transducer was measured with the copper wire.
10	The wire connected to the bottom of electrode of PZ29 was first thread through the housing before placing the transducer in the housing. The gold sputtered matching layer was facing towards the gold sputtered area of the housing. Superglue was used to bond the matching layer to the housing along the edges. After curing the superglue for approximately 30 minutes at room temperature, the electrical impedance of the transducer with wire and housing was measured.
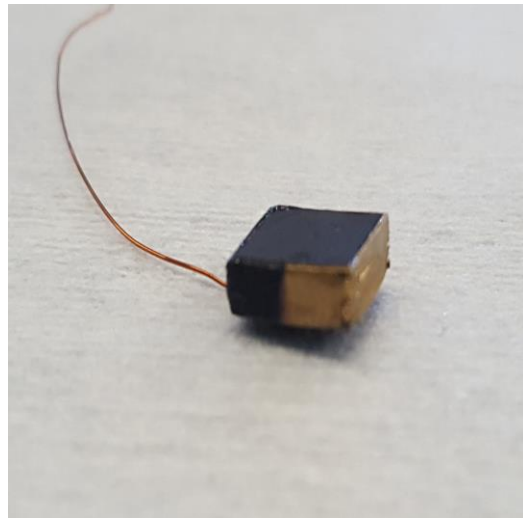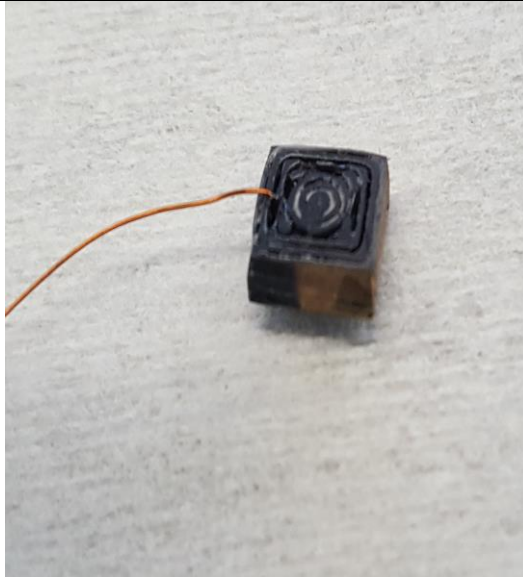
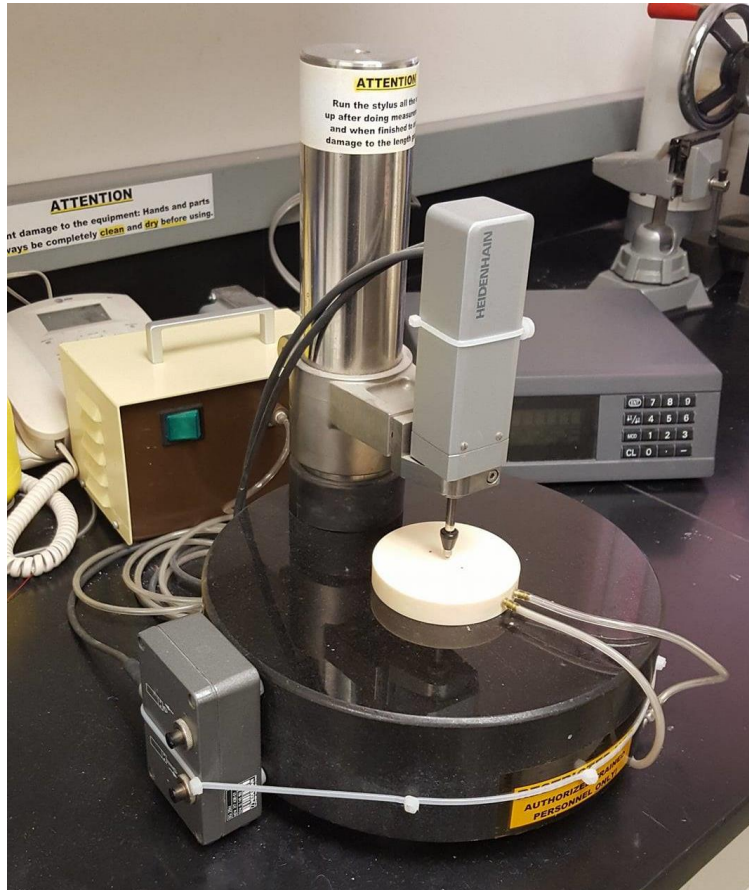| 11	A second copper wire was bonded to the sputtered side of the housing using silver epoxy to have contact with the top electrode. The bond was cured in the thermal chamber at 60 degrees for 4 hours.
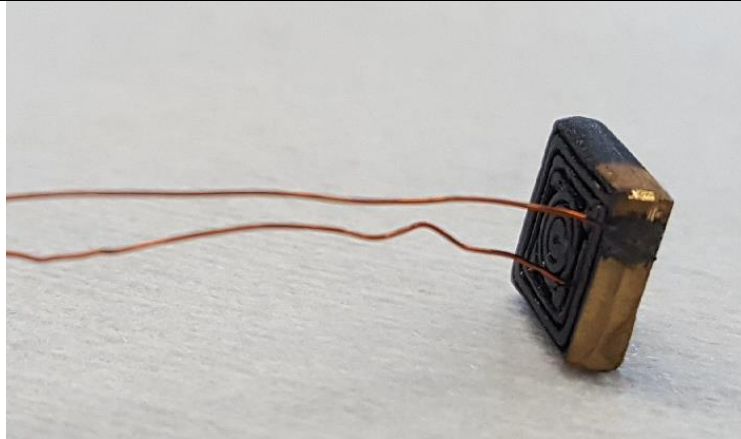
12	An electrical impedance measurement was done on the finished transducer.
13	To prepare the transducer for acoustic measurements in water, the transducer with housing was placed inside the 3D printed probe and sealed with DP460 3M epoxy.

B: Fabrication of High-Frequency Needle Transducers

Step	Explanation	Data
1	A large sample of PMN-PT was bonded to a glass plate and diced into multiple squares of 6mm*6mm using dicing saw Tcar 864-1 (Thermocarbon Inc. Casselberry, FL). After dicing, the smaller elements were removed from the glass plate and cleaned. The manual cleaning was done by hand using cotton swabs dipped in Trichloride (to remove wax), Acetone, Alcohol and deionized water. A sample of PZT-5H was manually cleaned.	<u>Material:</u> PMN-PT <u>Area:</u> 6mm*6mm <u>Material:</u> PZT-5H <u>Area:</u> 18mm*18mm

Cleaning station under fume hood. All cleaning was performed with cotton swabs.

Step	Explanation
2	A Heidenhain gauge system was used to measure the height deviation of a glass plate, allowing only 3µm deviation in height. The thickness gauge used in this lab is a Heindanhain measurement system (Heidenhain Corp. Schaumburg, IL). A Heidenhain Certo Length gauge is

|	combined with ND-287 digital readout. A ceramic vacuum suction plate is mounted on a Heidenhain CS-200 granite gauge stand. The ceramic suction plate is connected to a diaphragm pump. This system is highly accurate and will eliminate air gaps.
	Heidenhain measurement system.
3	Hotplate Mirak HP72620-26 (Barnstead/Thermolyne, Dubuque, IA) was used to wax bond the cleaned element to the glass at 70 degrees Celsius. The glass plate was stacked in a fixture, as seen in below, and placed in the Fisher Scientific Thermal Chamber at 60 degrees Celsius.

Fixture stack. From bottom: Bottom fixture, glass with wax bonded element, mylar, rubber, glass, tissue. The fixture is screwed to create uniform pressure on the piezoelectric element to reduce the wax thickness.

4	A lathe (Prazi SD-400 Powerturn Lathe. Plymouth, MA) cut spacers used to ensure even lapping. After cutting the spacers, they were lapped to a flat surface, manually cleaned, then glued to the edges of the glass. The spacers are necessary to ensure the element is lapped evenly. The element wax bonded to the glass plate with spacers on the sides was then lapped and polished to an even surface.
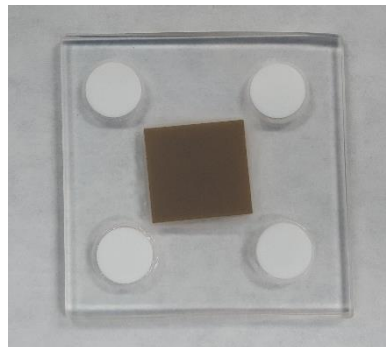
PZT-5H bonded to a glass plate with spacers near the corners.

Lapping station. All lapping was done by hand using sandpaper with different grainsize. The sandpaper was wetted with water at all times during lapping. Lapping was performed in a figure 8 pattern with rotation of the glass plate regularly.
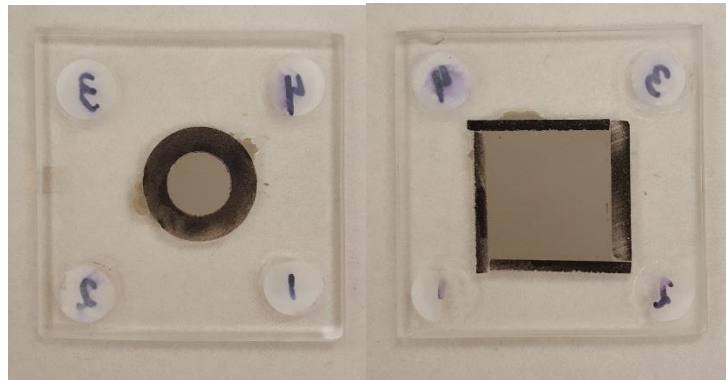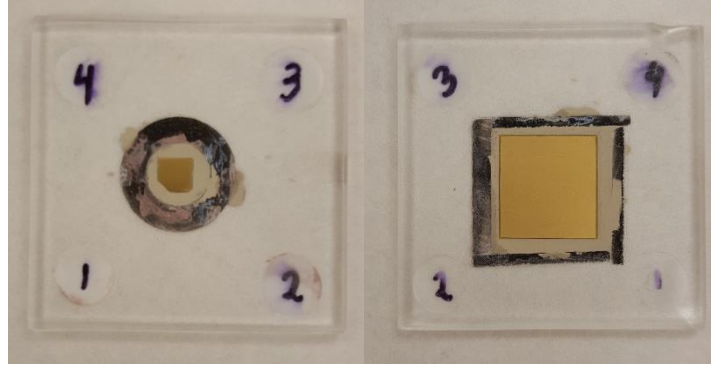
| 5	The sample was cleaned manually before Kapton tape was used to cover the glass, exposing only the surface of the element. Lab engineer, Ruimin Chen performed plasma cleaning using plasma treatment system PX-250 (Nordson MARCH. Concord, CA) before the element was sputtered with gold and chrome using NSC-3000 Sputter Coater (Nano-Master Inc. Austin, TX). The chrome serve as the seed layer for the gold which is one of the electrodes for the piezoelectric element.	Electrode
		Material:
		Cr-Au
		Thickness:
		Cr - 0.2µm
		Au – 0.5µm

| 6	After depositing the first electrode, the kapton tape could be removed. The element was released from the glass plate and cleaned. With the electrode facing down, the element was wax bonded to the glass plate. A new set of spacers were glued to the glass plate before the piezoelectric element was lapped and polished to the final thickness. Once again the sample was cleaned manually, plasma cleaned and the second electrode sputtered on element.	Thickness of PZT PMN-PT: 100µm Deviation: 1µm PZT-5H : 90µm Deviation: 0.3µm
7	The lathe was used to make a dam by cutting a rod aluminum silicate and drilling through the center, giving the damn an inner diameter 10mm and a height of 5mm. One side of the dam was lapped to an even surface and cleaned manually. The piezoelectric element was cleaned and wax bonded to a new piece of flat glass. The dam was then bonded with superglue to the glass plate with the lapped surface facing down and the element in the center. The dam was made to contain the silver epoxy, used for the first matching layer. Insulcure 9 and Insulcast 501 (Insulcast, ITW Engineered Polymers. Mongomeryville, PA) was measured in the ratio 1,3:10 and mixed before adding 3 grams of 2-3 silver particle powder for every 1.25 grams of epoxy mixture. The silver epoxy was deposited over the element inside the dam. To ensure an even distribution of the epoxy as well as the elimination of air bubbles in the silver epoxy, the sample was centrifuged for 15 minutes at 3000 RPM in the Allegra 6 Centrifuge machine (Backman Coulter Inc. Brea, CA). After centrifuging, the sample was cured at room temperature overnight, then	

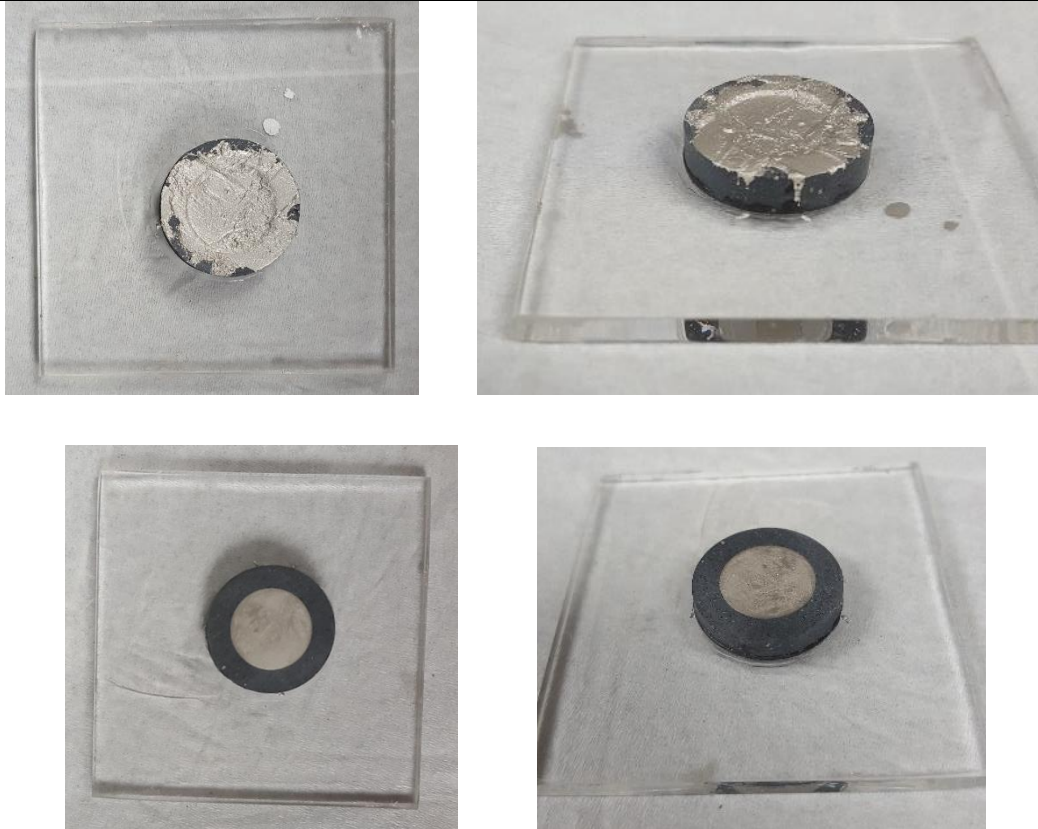|	in the thermal chamber at 40 degrees Celsius for 2 hours the next day.
	New spacers were cut and glued to the edge of the glass plate. The matching layer was lapped and polished to the final thickness.
8	The sample was then diced out of the damn, sacrificing a small area of the sides of the element. Using a razor blade, the left over dam and silver epoxy was carefully scraped off the glass before the element could be removed and manually cleaned.
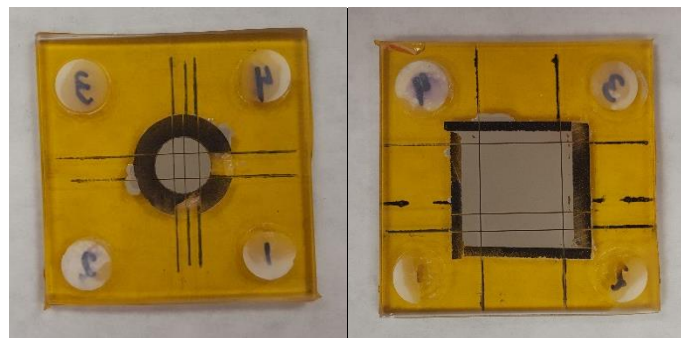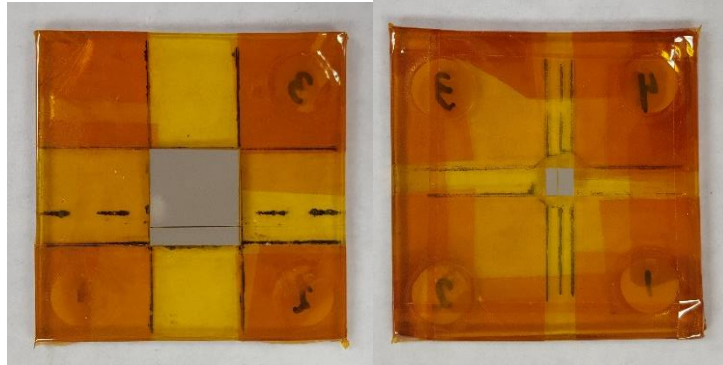
The largest pieces of the diced elements was used for a needle design for the transducers. A second fabrication approach was attempted, as described in 0

| 9 | The largest pieces of the diced elements was used for a needle design for the transducers. A second approach was attempted, as described in Appendix

The sample was then wax bonded to a piece of glass with the matching layer facing down. A new dam was made and superglued to the glass to contain the backing layer. Chemlok AP-131 (Lord Corp. Cary, NC) mixed in isopropanol was used as a primer to promote adhesion. The primer was deposited on the gold electrode using a cotton swab, then dried for 30 minutes in room temperature. E-solder 3022 (Von Roll Inc. New Haven, CT), a two component conductive silver epoxy, used for the backing material, was mixed in a ratio of 4 grams silver epoxy resin 0.32 grams Hardener. The mixture was deposited in the damn and centrifuged at 3000RPM for 15 minutes, left to dry overnight at room temperature, then cured for 2 hours at 40 degrees in the thermal chamber. E-solder will separate while curing, forming a thin layer of the non-conductive hardener towards the top which had to be lapped down to ensure the electrical connection to the back of the element. The sample was lapped past the non-conductive hardener. |

| 10 | The next step was to dice the elements. First, the sample was diced in slices with a 1.2 mm distance between each cut. The slices were then removed from the glass and wax bonded to a new glass plate with the side of the transducer facing down. The slices were diced into several parallelograms. The final elements were 1.2mm by 1.2mm with a 45 degree opening angle.

The housing for the transducers was cut from a cylinder of stainless steel with inner and outer diameter 1.75 and 2.05 respectively. One side of the housing was made flat, while the other was cut at 45 degrees. |
|---|---|
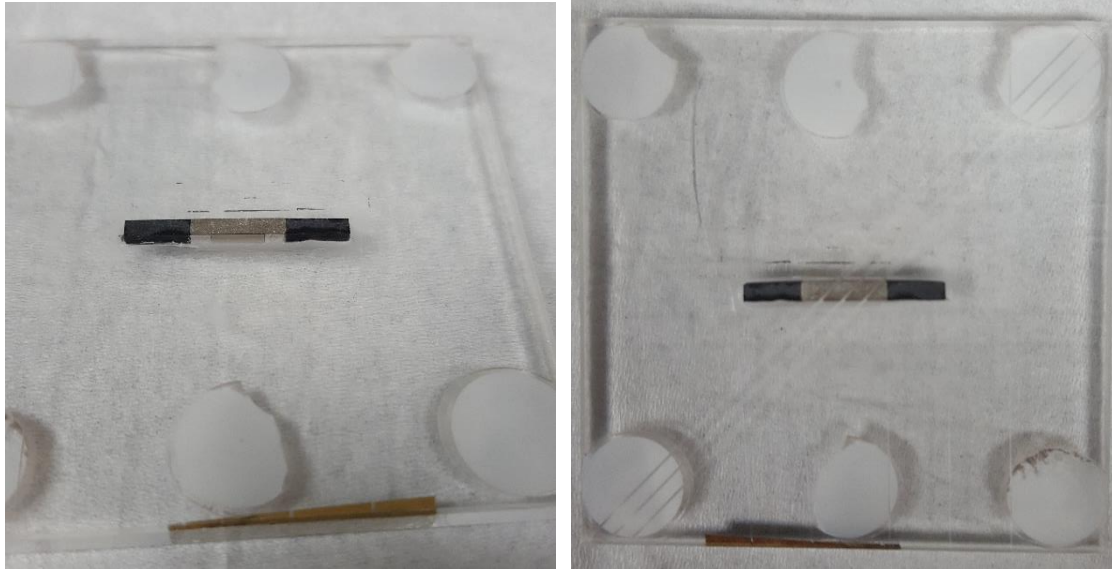
11	The element was then placed in a polymide tube with a wire bonded with E-solder 3022 to the conductive backing and left to cure overnight. The polymide tube provided electrical isolation from the needle housing.
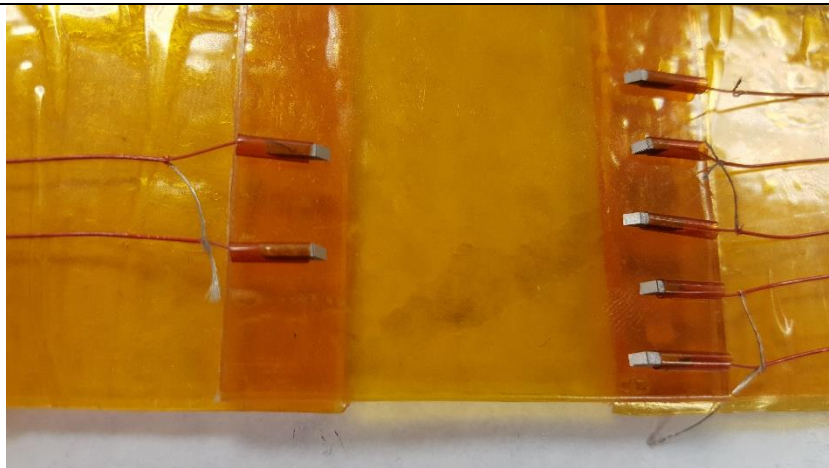
12	The element inside the polymide tube with a connected wire was then inserted into the housing. Epo-tek 301(Epoxy Technology Inc. Billerica, MA) was used to secure and isolate the element at the front of the housing. The two component epoxy was mixed in the ratio 4:1 of part A and B, respectively. The ground wire was bonded to the housing by E-solder 3022 and the transducers were left to cure in room temperature for 24 hours.
13	The transducers were manually cleaned before they were mounted to a glass plate with the footprint of the transducers lined horizontally. Kapton tape

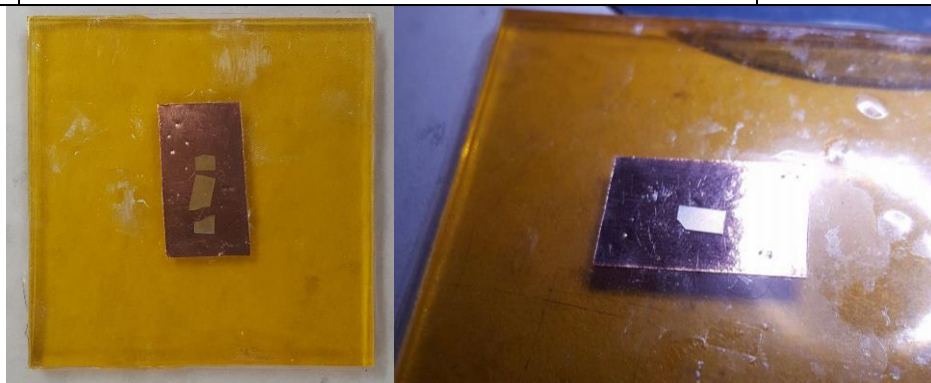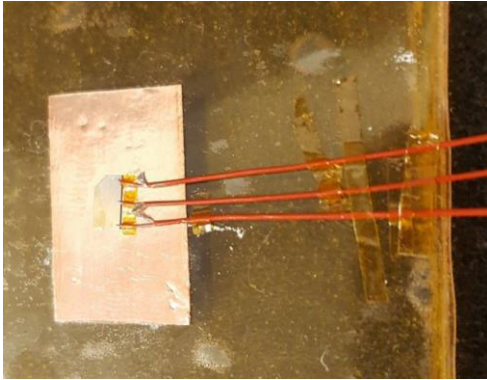|	
	secured the transducers to the glass plate, covering the bottom part of the housing. The mounted transducers were plasma cleaned and sputtered with gold to serve as the ground electrode for the transducers.
14	The second matching layer was made by evaporating 25µm thick layer of parylene, which coated the exposed parts of the transducer and housing.
15	The last step was to shorten the wire and strip the end. The wire was then connected to a ¼" SMA female-female adapter.

## C: Fabrication of High-Frequency Copper Sheet Transducers

| Step	Explanation	Data:
1-8	Fabrication steps 1-8 were the same as those described previously in table 1. Steps 9-15 describe the fabrication steps for a needle design	
16	The smaller element from the dicing described in step 8 was released from the glass plate and cleaned manually.	
17	A new flat glass plate was measured using the thickness gauge and cleaned. Adhesive dicing tape was used to cover the glass, this tape is adhesive on both sides, yet not as adhesive as double-sided tape. A small part of copper tape was cleaned on both sides to remove the adhesive. The cleaned tape was then placed on the dicing tape. Primer, AP-131 in isopropanol was applied with a cotton swab to promote adhesion. The primer was cured for 30 minutes in room temperature.	
	The transducer was bonded to the copper using only a small amount of E-solder. The E-solder being conductive would create a short circuit if the transducer was pressed to hard. The E-solder was cured in room temperature overnight and 2 hours at 40 degrees Celsius in the thermal chamber.	Copper thickness: 33µm E-solder thickness: 27-31µm

From left, PZT5-H and PMN-PT bonded to copper sheet on a glass plate with dicing tape.	
	Several coaxial cables were stripped and aligned along the length of the transducer, spaced approximately 1.2mm apart. The inner cable was connected to the conductive matching layer and the shield wire was connected to the copper. E-solder was used to bond the wires. The E-solder was cured in room temperature overnight and 2 hours at 40 degrees Celsius in the thermal chamber.

Wires aligned to sample prior to applying E-solder. Inner wire is in contact with top electrode, shielding wire is in contact with copper sheet and thereby bottom electrode.

	The edge of the copper was covered with kapton tape before sputtering 25 µm parylene over the surface of the transducer and the connected wires. The parylene serves as the second matching layer.	Parylene: 25µm
	The last step was to dice the transducer. The wires had been lined up prior to sputtering parylene to ensure the wires would not be cut during dicing. The dicing saw was programmed to dice 1.2mm*1.2mm squares. Due to the vibrations during dicing, the E-solder bonding layer released from the copper underneath on	Transducer surface area: 1.2mm*1.2mm

both the PZT-5H and PMN-PT transducer. Hence, there was no longer electrical connection to the bottom electrode of the transducer.

Due to limited time left in the USC ultrasound lab, this fabrication process was put on hold
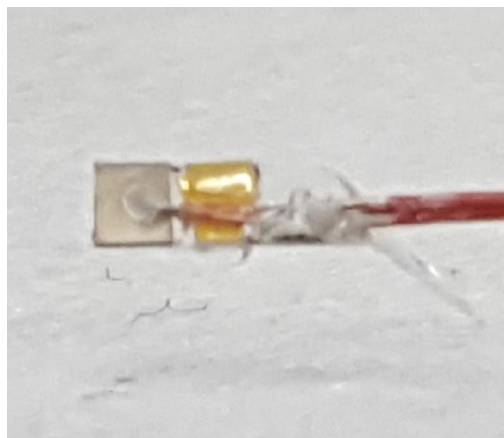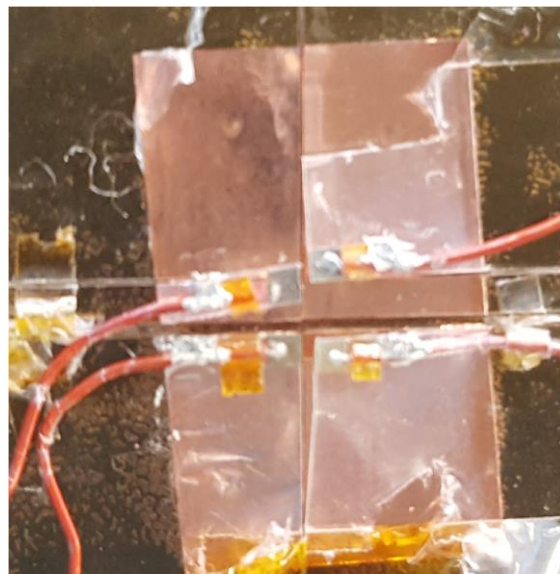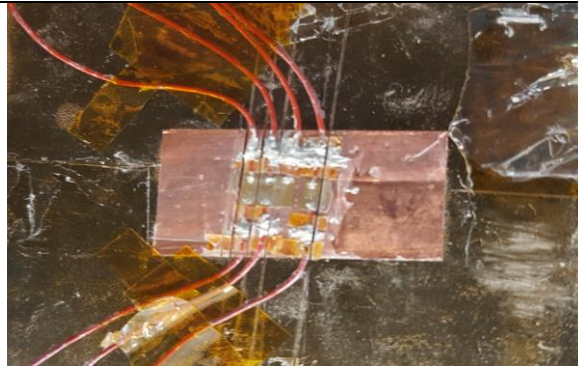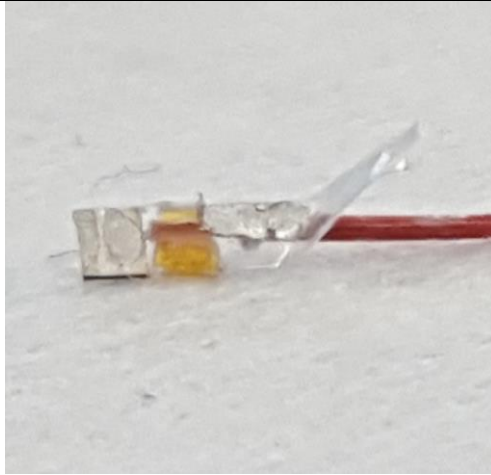
These transducers were supposed to be side facing.

This approach was not tested previously in the USC ultrasound lab. The thin piezoelectric element could possibly break due to the stress in the element during testing.

The copper and conductive epoxy under the transducer is large relative to bandwidth and would cause reflections and therefore a ringing effect. This was verified by the theoretical model

A mold of Sugru (Formformform. London UK), a moldable silicone rubber, would be made for the transducers to perform acoustic measurements.

Appendix D – PZ29 Ferroperm Data

Symbol	Pz29
$\varepsilon_{1,r}^{\sigma}$	2,44E+03
$\varepsilon_{3,r}^{\sigma}$	2,87E+03
$\varepsilon_{1,r}^{S}$	1,34E+03
$\varepsilon_{3,r}^{S}$	1,22E+03
tan $\delta\,(3^{\sigma})$	0,016
$T_C >$	235
k_p	0,643
k_t	0,524
k_{31}	0,370
k_{33}	0,752
k_{15}	0,671
e_{31}	-5,06
e_{33}	21,2
e_{15}	13,40
h_{31}	-4,68E+08
h_{33}	1,96E+09
h_{15}	1,13E+09
$Q_{m,p}^{E}$	76
$Q_{m,t}^{E}$	195
ρ	7,46E+03
c_{11}^{E}	1,34E+11
c_{12}^{E}	8,97E+10
c_{13}^{E}	8,57E+10
c_{33}^{E}	1,09E+11
$c_{44}^{E} = c_{55}^{E}$	1,85E+10
c_{66}	2,20E+10
c_{11}^{D}	1,36E+11
c_{12}^{D}	9,21E+10

c_{13}^{D}	7,58E+10
c_{33}^{D}	1,51E+11
$c_{44}^{D} = c_{55}^{D}$	3,36E+10